Atmos. Chem. Phys. Discuss., doi:10.5194/acp-2016-902, 2016
Manuscript under review for journal Atmos. Chem. Phys.
Published: 24 November 2016

Atmospheric Chemistry and Physics Discussions

3D evolution of Saharan dust transport towards Europe based on a 9-year EARLINET-optimized CALIPSO dataset

Eleni Marinou[1,2], Vassilis Amiridis[1], Ioannis Binietoglou[1,3], Stavros Solomos[1], Emannouil Proestakis[1,4], Dimitra Konsta[1], Athanasios Tsikerdekis[5], Nikolaos Papagiannopoulos[6], Georgia Vlastou[8], Prodromos Zanis[5], Dimitrios Balis[2], Ulla Wandinger[7], and Albert Ansmann[7]

[1]IAASARS, National Observatory of Athens, Athens, 15236, Greece
[2]Department of Physics, Aristotle University of Thessaloniki, Thessaloniki, 54124, Greece
[3]National Institute of R&D for Optoelectronics, Magurele, Romania
[4]Laboratory of Atmospheric Physics, Department of Physics, University of Patras, 26500, Greece
[5]School of Geology, Aristotle University of Thessaloniki, Thessaloniki, 54124, Greece
[6]Consiglio Nazionale delle Ricerche, Istituto di Metodologie per l'Analisi Ambientale (CNR-IMAA), Tito Scalo (PZ), Italy
[7]Leibniz Institute for Tropospheric Research, Leipzig, 04318, Germany
[8]Department of Physics, National and Kapodistrian University of Athens, Athens, Greece

Correspondence to: Eleni Marinou (elmarinou@noa.gr)

Abstract. In this study we utilize a new dust product developed using CALIPSO observations and EARLINET measurements and methods to provide a 3D multiyear analysis on the evolution of Saharan dust over North Africa and Europe. The product utilizes CALIPSO L2 backscatter product corrected with a depolarization-based method to separate pure dust in external aerosol mixtures and an adjusted Saharan dust lidar ratio based on long-term EARLINET measurements. The methodology is applied on a nine-year CALIPSO dataset (2007-2015) and the results are analysed here to reveal for the first time the 3D dust evolution and the seasonal patterns of dust over its transportation paths from the Sahara towards the Mediterranean and Continental Europe. During spring, dust is uniformly distributed in the horizontal over the Sahara desert. The dust transport over the Mediterranean Sea results on mean Dust Optical Depth (DOD) values of 0.1. During summer, the dust activity is mostly shifted to the western part of the desert where mean DOD near the source is up to 0.6. Elevated dust plumes with mean extinction values between 10 - 75 Mm^{-1} are observed throughout the year at various heights between 2 - 6 km, extending up to latitudes of 40° N. Dust advection is identified even at latitudes of about 60° N, but this is due to rare events of episodic nature. Dust plumes of high DOD are also observed above Balkans during winter period and above North-West Europe during autumn at heights between 2 - 4 km, reaching mean extinction values up to 50 Mm^{-1}. The dataset is considered unique with respect to its potential applications, including the evaluation of dust transport models and the estimation of cloud condensation and ice nuclei concentration profiles (CCN/IN). Finally, the product can be used to study dust dynamics during transportation, since it is capable of revealing even fine dynamical features such as the particle uplifting and deposition on European mountainous ridges such as Alps and Carpathian.

Atmos. Chem. Phys. Discuss., doi:10.5194/acp-2016-902, 2016
Manuscript under review for journal Atmos. Chem. Phys.
Published: 24 November 2016

Atmospheric Chemistry and Physics Discussions

1 Introduction

Mineral dust is ubiquitous in the atmosphere and one of the main contributors to the global aerosol burden (Zender et al., 2004; Textor et al., 2006), with almost half of the global dust emissions generated in Africa (Huneuus et al., 2011). This has large consequences for air quality downwind (Viana et al., 2002; Gobbi et al., 2007) as well as for the radiative budget due to scattering, absorption, and emission of solar and terrestrial radiation (Balkanski et al., 2007) and the cloud formation and lifetime (e.g., DeMott et al., 2003; Levin et al., 2005; Koren et al., 2010). The nature of these effects depends strongly on the vertical distribution of dust. For example, the absorbing dust particles will have a stronger impact on shortwave radiation when they are located above bright clouds (Yorks et al., 2009; Winker et al., 2013). Moreover, dust's atmospheric lifetime is much larger in the free troposphere than in the planetary boundary layer. Upon entering the free troposphere, dust particles can be transported across vast areas, altering the geographic pattern of their impacts (Prospero and Lamb, 2003; Levin et al., 2007; Ridley et al., 2012). Finally, the dust vertical distribution is crucial for dust-cloud interaction studies (e.g., Mamouri and Ansmann, 2016). Therefore, observing, monitoring and quantifying atmospheric dust burden and especially its vertical distribution is an important step towards understanding the climatic role of dust (IPCC, 2013, WG1, chapters 5, 7 and 9).

Lidar is the most prominent tool for aerosol profiling and has largely contributed to our knowledge of the vertical distribution of the dust optical properties (e.g., Liu et al. 2002; Ansmann et al., 2003; Balis et al., 2003; Papayannis et al., 2008; Mona et al., 2012). Polarization sensitive observations greatly expand the capabilities for dust detection employing remote sensors, as non-spherical dust particles have a distinct signature on the particle depolarization ratio (e.g., Liu et al., 2008; Tesche et al., 2009). In Europe, the European Aerosol Research Lidar Network (EARLINET; Pappalardo et al., 2014) operates sophisticated lidar systems employing depolarization techniques that have been invaluable for dust research. Advanced methodologies developed in EARLINET allow the complete characterization of different aerosol types including dust (e.g., Papayannis et al., 2008) but also the discrimination of dust contribution to the total aerosol load (Tesche et al., 2009).

The Cloud-Aerosol Lidar and Infrared Pathfinder Satellite (CALIPSO) mission equipped with the Cloud-Aerosol Lidar with Orthogonal Polarization (CALIOP) instrument has been delivering global aerosol and cloud profiles for more than ten years now (Winker et al., 2009). This dataset offers the possibility to characterize the three-dimensional distribution of aerosol as well as its temporal and spatial variation. CALIPSO has been established as an accurate and robust means of identifying mineral dust from space (Liu et al., 2008; Omar et al., 2009). The application of EARLINET methodologies on CALIPSO observations can improve the observations for mineral dust research, as already suggested and applied in Amiridis et al. (2013). Specifically, this study retrieves a pure dust extinction with high accuracy from CALIPSO, applying the depolarization-based separation method introduced by Tesche et al. (2009), coupled with the inference of a regionally uniform climatological LR (lidar ratio) for calculating dust extinction. This later value comes from long-term EARLINET measurements (Wandinger et al., 2010; Baars et al., 2016). It has been shown that the EARLINET-optimized CALIPSO dust product is in better agreement with Aerosol Robotic Network (AERONET) collocated measurements over Sahara and

Atmos. Chem. Phys. Discuss., doi:10.5194/acp-2016-902, 2016
Manuscript under review for journal Atmos. Chem. Phys.
Published: 24 November 2016

Europe and with Moderate Resolution Imaging Spectroradiometer (MODIS) measurements over the Mediterranean for collocated cells with low cloudiness (Amiridis et al., 2013). The product is considered as the first accurate dust retrieval from space, since dust discrimination methods applied on passive sensors are based on the separation of the fine from coarse particle mode (e.g., Kaufman et al., 2005), delivering mostly biased DODs over the oceans due to the contamination of the coarse mode by sea-salt particles (Su et al., 2013). One more advantage of the EARLINET-optimized CALIPSO dust product is its capability to provide equally-accurate dust retrievals over all surface types, as the Cloud-Aerosol Lidar with Orthogonal Polarization (CALIOP) utilizes its own light source, overcoming surface reflectance limitations of passive sensors (e.g., Hsu et al. 2004; Sayer et al., 2012).

Many studies utilized satellite observations to study dust over the Mediterranean during the last 15 years. Most of them focused on the horizontal dust distribution using passive remote sensing techniques. Specifically, Aerosol Optical Depth (AOD) data and other columnar aerosol properties have been used extensively to study dust using satellites such as SeaWIFS (Sea-Viewing Wide Field-of-View Sensor; Antoine and Nobileau, 2006), TOMS (Total Ozone Mapping Spectrometer; e.g., Alpert and Ganor, 2001; Israelevich et al., 2002), MODIS (Moderate Resolution Imaging Spectroradiometer; e.g., Barnaba and Gobbi, 2004; Papayannis et al., 2005; Kosmopoulos et al., 2008; Papadimas et al., 2008), OMI (Ozone Monitoring Instrument; e.g., Marey et al., 2011) and MISR (Multi-angle Imaging SpectroRadiometer; e.g., Marey et al., 2011). 3D dust observations from CALIPSO are used occasionally for case studies analyses (e.g., Amiridis et al., 2009; Mamouri et al., 2009; Marey et al., 2011; de Meij et al., 2012; Nabat et al., 2012, 2013; Mamouri and Ansmann, 2015). Winker et al. (2013) provided a 3D global aerosol climatology from CALIPSO. Moreover, several studies offered a global view of dust using CALIPSO (Liu et al., 2008a, 2008b; Adams et al., 2012; Yang et al., 2012; Tsamalis et al., 2013; Huang et al., 2015a, 2015b; Gkikas et al., 2015). In particular, the studies of Liu et al. (2008b), Yang et al. (2012) and Tsamalis et al. (2013) examined the transatlantic Saharan dust transport focusing on the optical properties of dust, the influence of nearby clouds and the vertical distribution of the Saharan Air Layer (SAL) respectively. Huang et al. (2015a) assessed the inferred most probable heights of global dust and introduced a separation method (Huang et al., 2015b) of anthropogenic dust (produced by human activities on disturbed soils) and free-tropospheric dust using CALIPSO and MODIS products. The studies of Liu et al. (2008a), Adams et al. (2012) and Gkikas et al. (2015) used CALIPSO observations in order to demonstrate the vertical structure of dust globally or above the Mediterranean respectively. All the aforementioned studies were based on standard CALIPSO products which have known limitations in accurately typing and quantifying the optical properties of pure dust (Wandinger et al., 2010; Tesche et al., 2013). One study used the EARLINET-optimized dust CALIPSO product to apply aerosol typing on MODIS and derive an aerosol climatology over the Eastern Mediterranean (Georgoulias et al., 2016). To our knowledge, large scale statistics of discriminated and optimized dust extinction and AOD fields from CALIPSO have not been provided to the literature yet. This paper aims to bridge this gap focusing on the vertical distribution of Saharan dust over North Africa and its transport towards Europe. The study domain is from 20° to 60° N and from 20° W to 30° E. More specifically, the 3D inter-seasonal variation and intensity of dust transport patterns above this region are investigated along with the inter-annual variations.

Atmos. Chem. Phys. Discuss., doi:10.5194/acp-2016-902, 2016
Manuscript under review for journal Atmos. Chem. Phys.
Published: 24 November 2016

Atmospheric Chemistry and Physics Discussions

The paper is organized as follows: In Sect. 2 the CALIPSO lidar data are briefly introduced and the pure dust retrieval scheme is described in detail. In Sect. 3, the main findings are presented and discussed. Initially, the inter-seasonal variation and intensity of dust transport patterns are examined and information on dust layer heights are presented (Sect. 3.1-3.3) followed by representative extinction coefficient values inside the dust plumes (Sect. 3.4). In Sect. 3.5, the inter-annual variation of dust is presented while our summary and concluding remarks are given in Sect. 4.

2 Data and methodology

2.1. CALIPSO product

CALIOP, flying on-board the joint NASA/CNES CALIPSO satellite, delivers global aerosol and cloud profiles since June 2006 (Winker et al., 2009). CALIOP measures aerosol backscatter profiles at 532 nm and 1064 nm, including parallel and perpendicular polarized components at 532 nm, at high horizontal and vertical resolution. These data are processed to Level 2 (L2) products, including aerosol and cloud backscatter and extinction coefficients at 532 nm and 1064 nm as well as the linear particle depolarization ratio at 532 nm (Winker et al., 2009). The processing algorithm, incorporated in the retrieval of the optical properties, separates the atmospheric scene in distinct atmospheric layers (i.e. aerosol, cloud, surface returns; Vaughan et al., 2009). For each aerosol layer the algorithm determines an aerosol subtype (i.e. dust, polluted dust, clean continental, polluted continental, marine, and smoke) based on a combination of information, such as the surface type, the layer integrated attenuated backscatter, the depolarization ratio at 532 nm and the aerosol layer height (Omar et al., 2009). The inferred subtype is used to assign the appropriate lidar ratio for each atmospheric altitude, a crucial input for the subsequent aerosol extinction retrieval (Young and Vaughan, 2009). Finally, the L2 products are aggregated to a gridded monthly-mean Level 3 (L3) product, providing mean profiles of extinction at 532 nm and mean AOD at a 2° × 5° spatial grid resolution (Winker et al, 2013). The most recent version of the L3 product (Version 3), released in October 2015, includes corrected AOD calculation from cloudy scenes, improved averaging of individual types as proposed by Amiridis et al. (2013) and Liu et al. (2008a), and corrections of signal artifacts responsible for high and low biases as also observed in Papagiannopoulos et al. (2016).

2.2. EARLINET-optimized CALISPO product

In this study, we make use of monthly averages at a horizontal resolution of 1° × 1° of the EARLINET-optimized pure dust extinction product, based on the methodology suggested by Amiridis et al. (2013). This product is one of the outcomes of the EARLINET-ESA collaboration to develop the LIVAS database (Amiridis et al., 2015). Unlike the original CALIPSO L3 product of 2° × 5° resolution, the 1 degree resolution of LIVAS has been proved very useful in supporting studies of the same spatial resolution, specifically retrievals from passive satellite sensors and model evaluation studies (e.g., Popp et al. 2016, Georgoulias et al., 2016, Tsikerdekis et al., 2016). In our methodology, the pure dust backscatter coefficient is decoupled from the total aerosol backscatter based on depolarization measurements, assuming a particle depolarization ratio

Atmos. Chem. Phys. Discuss., doi:10.5194/acp-2016-902, 2016
Manuscript under review for journal Atmos. Chem. Phys.
Published: 24 November 2016

(δ_p) value for pure dust equal to 0.31 (Tesche et al., 2009). Typical δ_p values measured by lidar methods for atmospheric dust in field campaigns around the globe are generally consistent with this value, independently of the source region, showing little variation (e.g., Sakai et al., 2000; Liu et al., 2008b; Freudenthaler et al., 2009; Groß et al., 2011; Burton et al., 2012; Burton et al., 2013; Groß et al., 2013; Groß et al., 2015; Illingworth et al., 2015). During SAMUM 1 and 2 campaigns Saharan dust δ_p values varied between 0.27 and 0.35 at 532nm (Ansmann et al., 2011), introducing negligible error in our calculations for the dust separated backscatter values. Based on this technique, we avoid the use of polluted dust and dust aerosol types used in CALIPSO, and thus, eliminate possible misclassifications found in CALIPSO L2 product (Burton et al., 2013). A final correction is related to the particle linear depolarization ratio, which is recalculated from L2 perpendicular and total backscatter profiles, to improve the accuracy compared to the original CALIPSO L2-Version 3 product which has a known bug (Tesche et al., 2013; Amiridis et al., 2013).

The quality control procedures and filtering criteria applied in the dataset are summarized in Table 1. In brief, CALIPSO L3 version 3 screening procedure is followed (Winker et al., 2013; http://www-calipso.larc.nasa.gov/resources/calipso_users_guide/data_summaries/l3/CALIOP_L3Products_3-00_v01.php), and additional filters are inserted to ensure the use of only cloud-free profiles. The additional methodology is as follows:

a) All profiles having cloud features anywhere in the column are also removed.

b) The profiles which fulfil the L3 CALIPSO "CAD score" or "Cirrus fringes" filters are removed (see also Table 1).

The pure dust extinction coefficient is computed by utilizing a lidar ratio of 55 sr instead of 40 sr used in the CALIPSO product (Omar et al., 2009; Lopes et al., 2013). This value is representative of dust over Europe, mainly originating from Northwest Africa, as measured in coordinated CALIPSO/EARLINET measurements (Pappalardo et al., 2010; Wanginder et al., 2011) and is in excellent agreement with recent studies of dust measurements both near the source (Tesche et al., 2009; Veselovskii et al., 2016) and during long range transport (Preißler et al., 2011; Kanitz et al., 2013; Gross et al., 2015; Baars et al., 2016; Papagiannopoulos et al., 2016). The individual backscatter coefficient profiles at 532 nm are aggregated at a horizontal spatial resolution of 1° × 1° and a vertical resolution of 60 m from -0.5 km to 20.2 km and 180 m from 20.2 km to 30.1 km. Height is referenced to above sea level (a.s.l.) altitudes.

2.3. Climatological vs Conditional dust product

In this study, we calculate two separate dust products, the climatological and the conditional:

The climatological dust product is based on Amiridis et al. (2013), where a value of 0 km^{-1} is assigned to the non-dust aerosol types when averaging within a cell. This product, hereinafter, is referred to as Climatological Dust Extinction (Clim-DE) and the corresponding AOD as Dust AOD (DOD), and is presented and discussed in Sect. 3.1-3.3. As already discussed in the introduction, this product has been evaluated against Aerosol Robotic Network (AERONET) and is in very good agreement with collocated measurements over Sahara and Europe (Amiridis et al., 2013) and the averaging methodology has been also adapted by L3, V3 CALIPSO product. The conditional dust product is calculated by averaging the CALIPSO dust extinction coefficients for all cases where dust is present, ignoring non-dust observations in the area. In particular, when

Atmos. Chem. Phys. Discuss., doi:10.5194/acp-2016-902, 2016
Manuscript under review for journal Atmos. Chem. Phys.
Published: 24 November 2016

deriving the mean dust extinction coefficient the clear air and non-dust aerosol types detected in the cell are ignored (set as NaN values when averaging). This product is referred to as Conditional Dust Extinction coefficient product (Con-DE) and is presented and discussed in Sect. 3.4.

The two products are provided for different applications. For example, Clim-DE is representative of the dust contribution to the total aerosol load. It can be used for climatological studies, especially when compared to the total AOD values of a region. For example, near-surface dust contribution given by this product could be used to provide estimates of the natural aerosol contribution to the total particle concentrations at surface for air-quality applications. The Con-DE product on the other hand, provides a measure of the intensity of the dust plumes. However, the dust extinction profiles reported for Con-DE should be used with caution, since they frequently exceed the total extinction values in a cell.

3 Results and discussion

In Sect. 3.1-3.4, we examine the inter-seasonal variation and intensity of dust transport patterns. In Sect. 3.1 we provide the average climatological state of the seasonal dust distribution at a spatial resolution of 1° × 1°. In Sect. 3.2 we give information on dust layer heights. In Sect. 3.3, we illustrate the mean climatological vertical structure of dust reaching Europe. To achieve that, the area of study is separated into five longitudinal zones with a step of 10°. In Sect. 3.4, we illustrate the vertical intensity of the dust plumes, using again longitudinal zone maps. Finally, in Sect. 3.5, we examine the inter-annual variation of dust.

3.1 Horizontal dust distribution

In this section, we provide the average climatological state of the seasonal horizontal dust distribution derived from CALIPSO dust product over period 2007-2015 at a spatial resolution of 1° × 1° for the domain of North Africa and Europe. The seasonal grouping used in this study is as follows: from January to March (JFM), from April to June (AMJ), from July to September (JAS) and from October to December (OND). In our study region, March and October are considered transition months for Saharan dust advection (e.g., Ganor, E., 1994; Guirado et al. 2014). This grouping is based on the dominant patterns revealed from the maps of monthly mean DODs (not shown). More specific, the decision is based on the observation that the events during February–March and October–November, although more rare, are usually more intense than those of the other months. This is further supported from ten year (2001 – 2011) analysis of African dust outbreak PM_{10} observations over the Mediterranean basin (Pey et al., 2013).

Figure 1 shows the geographical distribution of dust occurrences (Figs. 1a, c, e, g) and the corresponding mean DOD values (Figs. 1b, d, f, h) of each season. Based on Fig. 1, the overall percentages of dust occurrences and of the mean DOD values are larger during summer and spring months, while during autumn and winter the emission and transport of dust is suppressed (Israelevich et al., 2002; Schepanski et al., 2009). More specific, during JFM (Figs. 1a, b) limited dust activity is observed almost uniformly over the Sahara desert. The AOD remains roughly over the entire study domain below 0.2 with a

Atmos. Chem. Phys. Discuss., doi:10.5194/acp-2016-902, 2016
Manuscript under review for journal Atmos. Chem. Phys.
Published: 24 November 2016

Atmospheric Chemistry and Physics Discussions

standard deviation lower than 0.3. The dust occurrences decrease with latitude and the presence of dust is approximately 80 % over Africa and the Mediterranean region and decreases to lower than 50 % over northern Europe. The most affected area during these months is eastern Mediterranean. The cyclone formation over the central Mediterranean, which is affected by mid-latitude depressions generated either in the Atlantic Ocean or in north-western Europe (e.g., Trigo et al., 1999; Maheras et al., 2001), results in the transportation of dust from the Libyan Desert towards the Balkans which leads to dust occurrences up to 80 % (Fig. 1a) along with mean seasonal DOD of 0.1-0.2 (Fig. 1b). Similar mean values have been reported in the literature for this period, along with extreme events characterized by AOD values higher than 1 (Gerasopoulos et al., 2011). Moving northward, mean DOD tends to decrease due to the increasing distance from the major dust sources and also due to higher precipitation at the northern parts of the study region that efficiently removes dust from the atmosphere (e.g., Moulin et al., 1998; Marrioti et al., 2002).

During AMJ (Figs 1c, d) dust production occurring over the entire Saharan desert and mean DOD values exceeding 0.4 along with occurrences up to 80-90 % are found uniformly at latitudes between 20° N and 30° N. The activated dust sources are located in the broad "dust belt" and are usually associated with topographical lows in the arid regions, with land adjacent to strong topographical heights and with the intermountain basins (Prospero et al., 2002). The arrival of mid latitude extratropical cyclone systems from the Atlantic Ocean as well as cyclogenesis at the Gulf of Genoa and/or at northern African coast favours dust transport over central and eastern Mediterranean. Mean DOD at this area reaches values up to 0.15 (Fig. 1d) with standard deviation of 0.2 - 0.3. Dust is also present over central and northern Europe with occurrence percentages between 30 % and 50 % (Fig. 1c), revealing that dust particles can be transported far away from their sources under favourable meteorological conditions.

During JAS (Figs. 1e, f), intense dust activity is largely shifted to the western part of the Sahara where dust occurrences reach almost 100 % and mean DOD near the sources is up to 0.6. The migration of the ITCZ (Intertropical Convergence Zone) towards higher latitudes and the dominance of trade wind patterns (easterlies) benefit the transportation of dust towards the Atlantic Ocean as seen also by the westward plumes in Figs. 1e and 1f. Increased dust occurrences (up to 95 %) and mean DOD values (up to 0.2) during JAS are also found over western Mediterranean and South Italy.

During OND dust activity is significantly suppressed (Fig. 1g) except from the south-west desert areas close to the Sahel where mean DOD lies in the range 0.3-0.4 (Fig. 1h). The associated standard deviation is comparable to the DOD values. In general high values of DOD during spring and summer months over the dust sources correspond to high values of standard deviation up to 0.5. Low values of DOD over northern latitudes and during winter and autumn months are associated with low variations and the standard deviation is lower than 0.05.

3.2 Vertical dust distribution

CALIPSO offers the ability to assess the vertical distribution of dust from space. To facilitate the investigation of the vertical characteristics of dust, two parameters are introduced, the dust Top Height (TH) and the dust Centre of Mass height (CoM) (Mona et al., 2006; Mona et al., 2014; Binietoglou et al., 2015). TH is defined as the height corresponding to the altitude

Atmos. Chem. Phys. Discuss., doi:10.5194/acp-2016-902, 2016
Manuscript under review for journal Atmos. Chem. Phys.
Published: 24 November 2016

Atmospheric Chemistry and Physics Discussions

where the 98 % of the dust extinction lies below. CoM is estimated by the calculation of the extinction-weighted altitude given by the formula:

$$CoM = \frac{\int_{z_t}^{z_b} z a(z) dz}{\int_{z_t}^{z_b} a(z) dz}, \quad (1)$$

where z_b and z_t are the base and top altitude of the dust feature respectively. α denotes the aerosol extinction coefficient at altitude z. The estimate of CoM provides information related to the altitude where the most part of the dust load is located. This parameter is considered ideal for comparisons with aerosol layer height retrievals from passive remote sensing (e.g., IASI, GOME-2A, Sentinel5P and the future Sentinel-4 and Sentinel-5 missions (Ingmann et al. 2012)), since these retrievals are sensitive to the location of the dust mass maximum within the layer (e.g., TROPOMI Aerosol Layer Height product; Sanders et al. 2015).

Figure 2 shows the spatial distribution of TH and CoM for the four seasons. During JFM dust resides in general below 3 km a.s.e. (above surface elevation) over land with CoM at about 1 km a.s.e. (Figs. 2a, b). Over the sea, several transport paths are discernible especially over eastern Mediterranean with dust tops extending higher than2 km a.s.e. During AMJ, TH and CoM are up to 4.5 km and around 2 km a.s.e. respectively over eastern parts of Sahara. Over the Mediterranean Sea and South Europe dust tops extend around 2-3.5 km and CoM around 1-2 km a.s.e., with Centre and East Mediterranean having the most elevated plums (Figs. 2c, d). The latitudinal slope of CoM denotes the latitudinal transport of dust during AMJ from south to north. The highest TH values (>4.5 km) are found during the warm period (JAS) over north-western Africa and over the adjacent Atlantic Ocean region (Figs. 2e, f). This is most likely attributed to the intrusion of the lower tropospheric Atlantic monsoon, south of the ITCZ, and the development of MCS (mesoscale convective systems) that favour the elevation of dust at this area (Bou Karam et al., 2008). The dust height decreases towards the eastern part of the study region. In the interim, the dominance of the strong Saharan high enables the mobilization of dust from western part of Sahara towards western Mediterranean and Europe. This pattern leads to elevated dust between 2-4 km a.s.e. and CoM at ~1.5 km a.s.e. over south European countries and Balkans. During OND the situation is similar to JJA however with much lower heights (Figs. 2g, h).

3.3 Vertical dust cross sections

To further illustrate the vertical dynamics of dust reaching Europe, the area of study between 20° W and 30° E is separated into five longitudinal zones of 10° interval, covering latitudes from 20° to 60° N. The vertical structure of the averaged Climatological Dust Extinction coefficient (Clim-DE) for each of these five longitudinal zones (illustrated in Fig. 3 as latitude-height cross-sections) reveal several dust layers and strong seasonal variations. The two dashed lines are drawn such as to show how many dust observations are averaged for the extinction retrievals. The extinction values below the higher dashed line have been calculated by averaging a number of dust observations, greater than 18 (2 dust overpasses per season and year). The extinction values below the lower dashed line have been calculated by averaging a number of dust observations greater than 54 (2 dust overpasses per month and year). The median surface elevation is depicted with black

Atmos. Chem. Phys. Discuss., doi:10.5194/acp-2016-902, 2016
Manuscript under review for journal Atmos. Chem. Phys.
Published: 24 November 2016

Atmospheric Chemistry and Physics Discussions

colour. In general dust is always ubiquitous at heights close to the surface throughout the year. The lower layers are representative of near source dust activity and boundary layer processes. The spring and summer peaks indicate a mobilisation of the dust sources in the area during these months (Moulin et al., 1998; Schepanski et al., 2007). More specific, for the area between 10° W and 20° W over the Atlantic extending from Africa to west of Spain and England, the presence of elevated dust plumes is evident (Figs. 3a-d) mainly during summer and for latitudes up to 30°N. During JFM the plume is located below 2 km height a.s.l. (above sea level), while from spring to autumn the plume reaches a height of 5 km a.s.l. and yields high values of extinction coefficient (~75 Mm^{-1}) over Africa. Over the area from 0° to 10° W, extending from western Algeria, Morocco, Spain, and England we found Clim-DE values inside the Africa mixing layer greater than 50 $Mm^{-1}$for all seasons. Maximum values of extinction are observed during summer months when dust is elevated up to 6 km with Clim-DE values exceeding 200 Mm^{-1} (Fig. 3g). These findings are in good agreement with more than two years of AERONET observations in Tamanrasset site, a strategic site for dust research located in the heart of Sahara (Guirado et al., 2014). A steep decrease in extinction values is observed along African coastline with values of 20 Mm^{-1} above the southern part of the Iberian Peninsula (38°-42° N) where dust is trapped by the Pyrenees. At higher latitudes, the CALIPSO dust extinction is drastically reduced but still observed in ranges of 1-2 km a.s.l. Moving eastwards (0°-10° E) dust extends as far as the North Sea (50°-60° N) with mean Clim-DE values of 5 Mm^{-1} (Figs. 3i-j). Elevated dust is trapped topographically by the Alps (47°-52° N) with significantly high values >10 Mm^{-1}. As the dust-laden air-masses approach the mountains, they decelerate and thus the dust concentration increases (Israelevich et al., 2012). Maximum values of extinction (>50 Mm^{-1}) are observed over northern Africa during summer (Fig. 3k). Close to the Algerian sources, south of the Atlas Mountains (~30° N) extinction coefficient is greater than 200 Mm^{-1}close to the surface (Fig. 3k). As dust extends to higher latitudes (30°-40° N) Clim-DE decreases (<75 Mm^{-1}). Over the area between 10°-20° E (Figs. 3m-p), similar patterns are observed. This region includes the dust sources of Libya and central Sahara, central Mediterranean, the eastern Alps and part of North Europe. It is evident from this figure that dust extinction over central Mediterranean (35°-45° N) is around 25 Mm^{-1}throughout the year. As in the previous western zonal section the same pattern over the Alps is encountered. Moving further eastwards maximum values of Clim-DE are found during spring. At the most eastern part of the study area (20°-30° E; Figs. 3q-t), dust is trapped by the Carpathian Mountains (45°-49°N) especially during winter, thus highlighting, once more, the role of topography. Significant dust presence is evident all over the zonal section (until 60° N) mostly attributable to elevated dust traveling along with the westerlies from western and central parts of Europe towards East. The values of Clim-DE are higher (>45 Mm^{-1}) over Africa during winter and spring, and reach higher altitudes (5-6 km a.s.l.) during spring and summer. In summary, the obtained cross-sections for the five longitudinal zones indicate that higher extinction coefficient values are observed near the source and at low altitudes, where dust particles are efficiently deposited. The dominant Clim-DE values are >45 Mm^{-1} above Africa throughout the year and >75 Mm^{-1} above West Africa during JAS. In South Europe and Mediterranean, the dominant values are >10 Mm^{-1} in the first 2 km a.s.l. and ~30 Mm^{-1} close to the surface. For latitudes greater than 45° N, values around 5 Mm^{-1} are the most common.

Atmos. Chem. Phys. Discuss., doi:10.5194/acp-2016-902, 2016
Manuscript under review for journal Atmos. Chem. Phys.
Published: 24 November 2016

Atmospheric Chemistry and Physics Discussions

The above results can be used to estimate also the airborne mass concentration of dust and the impact on cloud formation. The dust mass concentration M_d can be obtained from the optical properties of dust using the following relationship (Mamouri and Ansmann, 2014):

$$M_d = \rho_d(v_d/\tau_d)a_d \quad (2)$$

Dust particle density, ρ_d, is assumed to be 2.6 g cm^{-3} (Ansmann et al., 2012). The conversion factor for dust volume to extinction ratio, v_d/τ_d, is assumed to be 0.64 x 10^{-6} m (Mamouri and Ansmann, to be submitted in AMT SALTRACE SI). a_d is the dust extinction coefficient.

For example, the Clim-DE values imply dust mass concentration >75 $\mu g\, m^{-3}$ above Africa throughout the year and >125 $\mu g\, m^{-3}$ above West Africa during JAS. In South Europe and Mediterranean, the corresponding values are >17 $\mu g\, m^{-3}$ in the first 2 km a.s.l. and ~50 $\mu g\, m^{-3}$ close to the surface. For latitudes greater than 45° N, values around 8 $\mu g\, m^{-3}$ are the most common.

Nevertheless, the decreasing intensity with height and latitude may not be representative for the dust episodes over Europe since the extinction coefficient values presented in Fig. 3 result from the mean of dust and non-dust episodes. In order to address this issue, the Con-DE is discussed in the next section.

3.4 Conditional dust cross sections

In this section we examine the Conditional Dust Extinction coefficient (Con-DE) distribution. The two dashed lines in Fig. 4 correspond to the number of dust observations greater than 18 (2 dust overpasses per season and year) and greater than 54 (2 dust overpasses per month and year) for the lower and higher dashed line respectively. Con-DE values derived from less than 4 dust observations in each cell are masked with grey colour (NaN values). The median surface elevation is depicted with black colour. Con-DE values are significantly different from the Clim-DE, as seen in Fig. 3. Although Con-DE has similar values to Clim-DE near the sources, where dust is always present, above the Atlantic and the Mediterranean Con-DE is characterized by significantly higher values. In the vertical cross sections of Fig. 4 the pattern of Con-DE shows two distinct populations of dust. For example over the longitudinal zone from 20° to 30° E during summer (Fig. 4o) two dust populations are visible: one above North Africa extending from the surface to ~5 km a.s.l. and another above the Mediterranean between 3 and 6 km a.s.l. The two distinct layers, also identified in other regions and in other seasons, are due to two different processes: the near surface dust at the southern parts of the study region represents fresh emissions from the dust sources, while the elevated plumes that extend northern until 40° N are due to the advection of dust, associated to the seasonality of the long-range transport paths (Lelieveld et al., 2002; Israelevich et al., 2012). This separation is enhanced as one move from the west to the east sectors. At the western part of the domain (10°-20° W) the near surface and elevated dust originates probably from the same sources. As the two layers diverge (10° W to 30° E) it is likely that the surface and elevated dust have different origins (e.g. West Sahara, Bodélé, East Sahara). Similar double layer patterns are found in all seasons and over all areas with various characteristics. For example during JAS at the region extending from 0° to 10° W (Fig. 4g) the generation of dust from the source region is much more intense than the transportation term, which is also evident. For the

Atmos. Chem. Phys. Discuss., doi:10.5194/acp-2016-902, 2016
Manuscript under review for journal Atmos. Chem. Phys.
Published: 24 November 2016

Atmospheric Chemistry and Physics Discussions

same period, in the area 0° to 10° E the transportation term above the Mediterranean between 3 and 6 km height, originating from the intensive source regions, becomes much more important than the source term at the same cross section.

The use of the particle depolarization ratio as a mean of estimating the age of dust from its state of mixing is supported by Fig. 5. Again, the two dashed lines in the figure correspond to the number of exceedances (NoE), NoE>18 and NoE>54. Particle depolarization ratio values derived from less than 4 dust observations in each cell are masked with grey colour (NaN values) and the median surface elevation is depicted with black colour. In Fig. 5 we see the mean depolarization corresponding to Fig. 4. As it can be seen, the depolarization is higher for air masses closer to the desert while it decreases as the air-masses travel towards Europe. This is due to the mixing of dust with other aerosol particles, which takes place after some days of transport. However, the depolarization ratio cannot be considered as a possible age index, since it provides the mixing of dust with other particles (Tesche et al., 2009). It is used here as an age estimator only because the Sahara desert is away from Europe and the mixing of transported dust with anthropogenic particles takes place as soon as the plumes mix with anthropogenic particles over the European Continent.

Looking in more detail the vertical cross sections of Fig. 4, we observe the rare but very intense elevated dust plums during JFM (4a, e, l, m). During that period, dust is advected between 1.5–4 km height a.s.l. with Con-DE values >45 Mm^{-1} equivalent to dust mass concentrations >75$\mu g\ m^{-3}$. Furthermore, in Fig. 4q, the intensity of the JFM dust episodes above the Balkans is depicted. The Con-DE value in this domain is in the same range with the one in the other regions at the same period, but the dust plumes can be thicker, extending from the ground until 4 km a.s.l. The trapping of Saharan dust from the mountainous ridges of Europe is also evident by the Con-DE cross-sections. Accumulation of dust at the windward slopes results after the deceleration of the transport air masses along the mountain ridges. Increased deposition rates at this areas result also in the formation of "brown snow" and albedo reduction, with profound climatological implications (e.g. Fujita, 2007; Shahgedanova et al., 2013). This phenomenon is more intense during JFM period due to the advection of dust in lower heights at this period.

During AMJ (4b, f, j, n, r) and JAS (4c, g, k, o, s) the elevated dust above Mediterranean has Con-DE values of 35-50 Mm^{-1} (58-83 $\mu g\ m^{-3}$), in heights between 2-6 km and up to latitudes of 40° N. For latitudes 40° and 50° N, during the warm seasons (AMJ and JAS), the Con-DE inside the transported dust plumes are between 20-40 Mm^{-1} everywhere (33-67 $\mu g\ m^{-3}$). Rare events, characterized by relatively higher Con-DE (>35 $Mm^{-1}$and >58 $\mu g\ m^{-3}$), between 2-5 km a.s.l., are observed over the British Isles and Germany during OND (Figs. 4h, i). These events, caused by the propagating low pressure systems over the East Atlantic, have been documented in detail from the EARLINET community reporting extinction coefficient values up to 200 Mm^{-1} inside dust plumes (Ansmann et al., 2003; Müller et al., 2003). In the vertical cross section of Fig. 4 is evident that dust reaches the upper levels of the troposphere (>8 km a.s.l.) with Con-DE values of ~10 Mm^{-1} in all longitudinal zones and during all seasons. Dust occurrence is very low, close to zero for heights greater than 8 km a.s.l. during spring and summer and for heights greater than 6 km a.s.l. during autumn and winter.

Atmos. Chem. Phys. Discuss., doi:10.5194/acp-2016-902, 2016
Manuscript under review for journal Atmos. Chem. Phys.
Published: 24 November 2016

3.5 Interannual variability of dust

In this section we utilize the CALIPSO derived monthly mean DOD values, for the total-column and for five individual layers (0.18–0.5, 0.5–1, 1–2, 2–4, 4–8 km), to study their inter-annual variability during the 9 year period between 2007 and 2015. The selected layers are representative for both near surface and long-range transported dust plumes. The data are aggregated on a 10° x 10° cell over the study region. Using a first-order autoregressive linear regression model on the de-seasonalized monthly DOD values as described in Zanis et al. (2006), temporal trends of DOD were calculated. Figure 6 shows the geographical distribution of de-seasonalized trends (year^{-1}) for the columnar DOD (a) and for the five individual layers (b-f). Hatched filled grid cells depict the statistical significance trends with 99% confidence. A decrease ~ 0.001 yr^{-1} (~ 4% yr^{-1}) is evident for the South European cells (0°-30° E, 40°–50° N) (with these values being > 95% statistical significant). Examination of the five vertical layers shows a similar decreasing pattern. The negative trends observed in the area (mainly above North Africa and Mediterranean), are additionally characterized by constant decrease throughout the layers, although the trends are not statistical significant. The small negative DOD trends (< 0.002 yr^{-1} corresponds to < 5% yr^{-1}) coming from this temporal limited dataset, are in good agreement with the global decrease of dust estimated from an 161-year time series of dust from 1851 to 2011, created by projecting wind field pattern onto surface winds from a historical reanalysis in Evan et al. (2016), and also with the global mean near-surface dust concentration decrease by 1.2% yr^{-1} reported in Shao et al. (2013) paleoclimate research for the period 1984-2012 (even though Europe and North America are excluded from their trend analysis). A possible increase is only found for west Sahara areas (10° - 0° W, 20°–30° N). However, the results for this cell are not considered statistical significant.

4. Summary and conclusions

An optimized CALIPSO dust product was recently developed with a regional correction of the Saharan dust LR using EARLINET measurements (Amiridis et al., 2013). The same product has been utilized here to provide the three-dimensional dust distribution and its transport pathways across northern Africa and Europe. The monthly climatology of African dust obtained from 2007 to 2015 allows the description of the spatio-temporal features of dust properties. The study of the mean state climatology shows strong seasonal shifts in dust source regions and transportation pathways. The seasonal cycle of the dust transport is well captured with the lowest values of DOD in winter and the highest values in spring and summer. During summer and autumn, dust aerosols are more confined to the source region, while during spring significant dust aerosols from the Sahara are extended uniformly over North Sahara and are transported over the Mediterranean and Europe. Dust extinction coefficient, Centre of Mass and Top Height retrieved parameters are used to quantitatively understand the 3D evolution of dust and the seasonal differences in the vertical distribution which are evident as well. Over the source region of Sahara Desert, dust CoM and the TH are higher during spring and summer and lowest during winter. Dust transport mechanisms are more efficient during summer when dust is often lifted up to 6 km, coinciding with the deepest dust layer. The appearance of localized regions of increased extinction coefficient values over mountains (the Alps, the Pyrenees, and

the Carpathian Mountains) denotes the existence of aerosol transport routes that decelerate in front of the mountain ranges. Rare and intense events are observed above Balkans during winter period and above North-West Europe during autumn. The inter-annual analysis revealed that DOD trends during the study period are of the order of 0.001/year for the South European cells, showing constant decrease throughout the different layers.

The dust climatology presented here is of paramount importance in understanding the three-dimensional production and transport of Saharan dust which will contribute to better estimate the dust impacts on climate. The use of two products, the climatological and conditional in this study allowed us to conclude on both the dust contribution to the total aerosol load over our domain, but also on the intensity of the Saharan dust events recorded in the region. Future work includes: (i) the optimization of CALIPSO dust retrievals based on measured dust LR from ground-based lidars and particle depolarization ratio over extended regions of deserts in the Middle East and China, to obtain a robust global climatology of dust; (ii) the calculation of cloud condensation nuclei and ice nuclei concentrations from polarization lidar as suggested by Mamouri and Ansmann (2016), to provide a quantification of the climatic effect of dust on cloud formation.

Acknowledgements

The authors acknowledge support through the following projects and research programs:

- ESA-ESTEC project LIVAS (contract N°4000104106/11/NL/FF/fk)
- BEYOND under grant agreement no. 316210 of the European Union Seventh Framework Programme: FP7-REGPOT-2012-2013-1
- MarcoPolo under grant agreement n° 606953 from the European Union Seventh Framework Programme (FP7/2007-2013)
- ACTRIS under grant agreement no. 262254 of the European Union Seventh Framework Programme: FP7/2007-2013
- ACTRIS-2 under grant agreement no. 654109 from the European Union's Horizon 2020 research and innovation programme
- ITaRS under grant agreement no. 289923 of the European Union Seventh Framework Programme: FP7/2007-2013
- ECARS under grant agreement No 602014 from the European Union's Horizon 2020 Research and Innovation programme
- EPAN II and PEP under the national action "Bilateral, multilateral and regional R&T cooperations" (AEROVIS Sino-Greek project)
- A. G. Leventis Foundation scholarship

The authors acknowledge EARLINET for providing aerosol lidar profiles available under the World Data Center for Climate (WDCC) (The EARLINET publishing group 2000-2010, 2014 a, b, c, d, e). We thank the AERONET PIs and their staff for establishing and maintaining the AERONET sites used in this investigation. CALIPSO data were obtained from the ICARE Data Center (http://www.icare.univ-lille1.fr/). CALIPSO data were provided by NASA. We thank the ICARE Data and

Services Center for providing access to the data used in this study and their computational center. We thank Jason Tackett for his support during the algorithm development for the production of Level 3 CALIPSO products.

References

Adams, A. M., Prospero, J. M., and Zhang, C.: CALIPSO-Derived Three-Dimensional Structure of Aerosol over the Atlantic Basin and Adjacent Continents, J. Climate, 25, 6862–6879, doi:10.1175/JCLI-D-11-00672.1, 2012.

Alpert, P., and Ganor, E.: Sahara mineral dust measurements from TOMS: Comparison to surface observations over the Middle East for the extreme dust storm, 14-17 March 1998, J. Geophys. Res., 106(D16), 18275–18286, doi:10.1029/2000JD900366, 2001.

Amiridis, V., Balis, D. S., Giannakaki, E., Stohl, A., Kazadzis, S., Koukouli, M. E., and Zanis, P.: Optical characteristics of biomass burning aerosols over Southeastern Europe determined from UV Raman lidar measurements, Atmos. Chem. Phys., 9, 2431-2440, doi:10.5194/acp-9-2431-2009, 2009.

Amiridis, V., Wandinger, U., Marinou, E., Giannakaki, E., Tsekeri, A., Basart, S., Kazadzis, S., Gkikas, A., Taylor, M., Baldasano, J., and Ansmann, A.: Optimizing CALIPSO Saharan dust retrievals, Atmos. Chem. Phys., 13, 12089-12106, doi:10.5194/acp-13-12089-2013, 2013.

Amiridis, V., Marinou, E., Tsekeri, A., Wandinger, U., Schwarz, A., Giannakaki, E., Mamouri, R., Kokkalis, P., Binietoglou, I., Solomos, S., Herekakis, T., Kazadzis, S., Gerasopoulos, E., Proestakis, E., Kottas, M., Balis, D., Papayannis, A., Kontoes, C., Kourtidis, K., Papagiannopoulos, N., Mona, L., Pappalardo, G., Le Rille, O., and Ansmann, A.: LIVAS: a 3-D multi-wavelength aerosol/cloud database based on CALIPSO and EARLINET, Atmos. Chem. Phys., 15(13), 7127–7153, doi:10.5194/acp-15-7127-2015, 2015.

Ansmann, A., Bösenberg, J., Chaikovsky, A., Comeron, A., Eckhardt, S., Eixmann, R., Freudenthaler, V., Ginoux, P., Komguem, L., Linne, H., Lopez Marquez, M. A., Matthias, V., Mattis, I., Mitev, V., Muller, D., Music, S., Nickovic, S., Pelon, J., Sauvage, L., Sobolewsky, P., Srivastava, M. K., Stohl, A., Torres, O., Vaughan, G., Wandinger, U., and Wiegner, M.: Long-range transport of Saharan dust to northern Europe: The 11–16 October 2001 outbreak observed with EARLINET, J. Geophys. Res., 108(D24), 4783, doi:10.1029/2003JD003757, 2003.

Ansmann, A., Petzold, A., Kandler, K., Tegen, I., Wendisch, M., Muller, D., Weinzierl, B., Muller, T., and Heintzenberg, J.: Saharan Mineral Dust Experiments SAMUM–1 and SAMUM–2: what have we learned?, Tellus B, 63, 403–429. doi: 10.1111/j.1600-0889.2011.00555.x., 2011.

Ansmann, A., Seifert, P., Tesche, M., and Wandinger, U.: Profiling of fine and coarse particle mass: case studies of Saharan dust and Eyjafjallajökull/Grimsvötn volcanic plumes, Atmos. Chem. Phys., 12, 9399–9415, doi: 10.5194/acp-12-9399-2012, 2012.

Antoine, D., and Nobileau, D.: Recent increase of Saharan dust transport over the Mediterranean Sea, as revealed from ocean color satellite (SeaWiFS) observations, J. Geophys. Res., 111, D12214, doi:10.1029/2005JD006795, 2006.

Baars, H., Kanitz, T., Engelmann, R., Althausen, D., Heese, B., Komppula, M., Preißler, J., Tesche, M., Ansmann, A., Wandinger, U., Lim, J.-H., Ahn, J. Y., Stachlewska, I. S., Amiridis, V., Marinou, E., Seifert, P., Hofer, J., Skupin, A., Schneider, F., Bohlmann, S., Foth, A., Bley, S., Pfüller, A., Giannakaki, E., Lihavainen, H., Viisanen, Y., Hooda, R. K., Pereira, S. N., Bortoli, D., Wagner, F., Mattis, I., Janicka, L., Markowicz, K. M., Achtert, P., Artaxo, P., Pauliquevis, T., Souza, R. A. F., Sharma, V. P., van Zyl, P. G., Beukes, J. P., Sun, J., Rohwer, E. G., Deng, R., Mamouri, R.-E., and Zamorano, F.: An overview of the first decade of PollyNET: an emerging network of automated Raman-polarization lidars for continuous aerosol profiling, Atmos. Chem. Phys., 16, 5111-5137, doi:10.5194/acp-16-5111-2016, 2016.

Balis, D. S., Amiridis, V.,Nickovic, S., Papayannis, A., and Zerefos, C.: Optical properties of Saharan dust layers as detected by a Raman lidar at Thessaloniki, Greece, Geophys. Res. Lett., 31, L13104, doi:10.1029/2004GL019881, 2004.

Balkanski, Y., Schulz, M., Claquin, T., and Guibert, S.: Reevaluation of Mineral aerosol radiative forcings suggests a better agreement with satellite and AERONET data, Atmos. Chem. Phys., 7, 81–95, doi:10.5194/acp-7-81-2007, 2007.

Ban-Weiss, G.A., Cao, L., Bala, G., and Caldeira, K.: Dependence of Climate Forcing and Response on the Altitude of Black Carbon Aerosols, Clim Dyn., 38, 897–911, doi:10.1007/s00382-011-1052-y, 2012.

Barnaba, F., and Gobbi, G. P.: Aerosol seasonal variability over the Mediterranean region and relative impact of maritime, continental and Saharan dust particles over the basin from MODIS data in the year 2001, Atmos. Chem. Phys., 4, 2367-2391, doi:10.5194/acp-4-2367-2004, 2004.

Binietoglou, I., Basart, S., Alados-Arboledas, L., Amiridis, V., Argyrouli, A., Baars, H., Baldasano, J. M., Balis, D., Belegante, L., Bravo-Aranda, J. A., Burlizzi, P., Carrasco, V., Chaikovsky, A., Comerón, A., D'Amico, G., Filioglou, M., Granados-Muñoz, M. J., Guerrero-Rascado, J. L., Ilic, L., Kokkalis, P., Maurizi, A., Mona, L., Monti, F., Muñoz-Porcar, C., Nicolae, D., Papayannis, A., Pappalardo, G., Pejanovic, G., Pereira, S. N., Perrone, M. R., Pietruczuk, A., Posyniak, M., Rocadenbosch, F., Rodríguez-Gómez, A., Sicard, M., Siomos, N., Szkop, A., Terradellas, E., Tsekeri, A., Vukovic, A., Wandinger, U., and Wagner, J.: A methodology for investigating dust model performance using synergistic EARLINET/AERONET dust concentration retrievals, Atmos. Meas. Tech., 8, 3577-3600, doi:10.5194/amt-8-3577-2015, 2015.

Bou Karam, D., Flamant, C., Knippertz, P., Reitebuch, O., Pelon, J., Chong, M. and Dabas, A.: Dust emissions over the Sahel associated with the West African monsoon intertropical discontinuity region: A representative case-study, Q.J.R. Meteorol. Soc., 134, 621–634. doi:10.1002/qj.244, 2008.

Burton, S. P., Ferrare, R. A., Vaughan, M. A., Omar, A. H., Rogers, R. R., Hostetler, C. A., and Hair, J. W.: Aerosol classification from airborne HSRL and comparisons with the CALIPSO vertical feature mask, Atmos. Meas. Tech., 6, 1397–1412, doi:10.5194/amt-6-1397-2013, 2013.

Charlson, R. J., Schartz, S.E., Hales, J.M., Cess, R.D., Coakley, J.A., Hansen, J.E., and Hofmann, D.J.: Climate Forcing by Anthropogenic Aerosols, Science, 255,423–430. doi: 10.1126/science.255.5043.423, 1992

Creamean, J.M., Suski, K.J., Rosenfeld, D., Cazorla, A., DeMott, P.J., Sullivan, R.C., White, A.B., Ralph, F.M., Minnis, P., Comstock, J.M., Tomlinson, J.M., and Prather, K.A.: Dust and biological aerosols from the Sahara and Asia influence precipitation in the western U.S, Science, 339, 1572–1578. doi:10.1126/science.1227279, 2013.

Darmenov, A., and Sokolik, I.N.: Identifying the regional thermal-IR radiative signature of mineral dust with MODIS,Geophys. Res. Lett., 32, L16803, doi:10.1029/2005GL023092, 2005.

de Meij, A. and Lelieveld, J.: Evaluating aerosol optical properties observed by ground-based and satellite remote sensing over the Mediterranean and the Middle East in 2006, Atmos. Res., 99, 415-433, doi:10.1016/j.atmosres.2010.11.005, 2011.

de Meij, A., Pozzer, A., Pringle, K. J., Tost, H., and Lelieveld, J.: EMAC model evaluation and analysis of atmospheric aerosol properties and distribution, Atmos. Res, 114-115, 38-69, doi:10.1016/j.atmosres.2012.05.014, 2012.

DeMott, P. J., Sassen, K., Poellot, M.R., Baumgardner, D., Rogers, D.C., Brooks, S.D., Prenni, A.J., and Kreidenweis, S.M.: African dust aerosols as atmospheric ice nuclei, Geophys. Res. Lett., 30, 1732, doi:10.1029/2003GL017410, 2003.

DeMott, P.J., Prenni, A.J., McMeeking, G.R., Sullivan, R.C., Petters, M.D., Tobo, Y., Niemand, M., Möhler, O., Snider, J.R., Wang, Z., and Kreidenweis, S.M.: Integrating laboratory and field data to quantify the immersion freezing ice nucleation activity of mineral dust particles, Atmos. Chem. Phys., 15, 393–409, doi:10.5194/acp-15-393-2015, 2015.

Dubovik, O., and King, M. D.: A flexible inversion algorithm for retrieval of aerosol optical properties from Sun and sky radiance measurements, J. Geophys. Res., 105(D16), 20673–20696, doi:10.1029/2000JD900282, 2000.

Dubovik, O., Sinyuk, A., Lapyonok, T., Holben, B. N., Mishchenko, M., Yang, P., Eck, T. F., Volten, H., Muñoz, O., Veihelmann, B., van der Zande, W. J., Leon, J.-F., Sorokin, M. and Slutsker, I.: Application of spheroid models to account for aerosol particle nonsphericity in remote sensing of desert dust, J. Geophys. Res., 111(D11), D11208, doi:10.1029/2005JD006619, 2006.

Evan, A. T., Flamant, C., Gaetani, M. and Guichard, F.: The past, present and future of African dust, Nature, 531(7595), 493–495, doi:10.1038/nature17149, 2016.

Freudenthaler, V., Esselborn, M., Wiegner, M., Heese, B., Tesche, M., Ansmann, A., Müller, D., Althausen, D., Wirth, M., Fix, A., Ehret, G., Knippertz, P., Toledano, C., Gasteiger, J., Garhammer, M., and Seefeldner, M.: Depolarization ratio profiling at several wavelengths in pure Saharan dust during SAMUM 2006, Tellus, Ser. B, 61, 165–179, doi:10.1111/j.1600-0889.2008.00396.x, 2009.

Fujita, K.: Effect of dust event timing on glacier runoff sensitivity analysis for a Tibetan glacier, Hydrol. Process., 21, 2892–2896, 2007.

Georgoulias, A. K., Alexandri, G., Kourtidis, K. A., Lelieveld, J., Zanis, P., Pöschl, U., Levy, R., Amiridis, V., Marinou, E., and Tsikerdekis, A.: Spatiotemporal variability and contribution of different aerosol types to the Aerosol Optical Depth over the Eastern Mediterranean, Atmos. Chem. Phys. Discuss., doi:10.5194/acp-2016-401, in review, 2016.

Gerasopoulos, E., Amiridis, V., Kazadzis, S., Kokkalis, P., Eleftheratos, K., Andreae, M. O., Andreae, T. W., El-Askary, H., and Zerefos, C. S.: Three-year ground based measurements of aerosol optical depth over the Eastern Mediterranean: the urban environment of Athens, Atmos. Chem. Phys., 11, 2145-2159, doi:10.5194/acp-11-2145-2011, 2011.

Gkikas, A., Basart, S., Hatzianastassiou, N., Marinou, E., Amiridis, V., Kazadzis, S., Pey, J., Querol, X., Jorba, O., Gassó, S., and Baldasano, J. M.: Mediterranean desert dust outbreaks and their vertical structure based on remote sensing data, Atmos. Chem. Phys. Discuss., 15, 27675-27748, doi:10.5194/acpd-15-27675-2015, 2015.

Gobbi, G., Barnaba, F., and Ammannato, L.: Estimating the impact of saharan dust on the year 2001 PM10 record of Rome, Italy, Atmospheric Environment, 41, 261–275, doi:10.1016/j.atmosenv.2006.08.036., 2007.

Groß, S., Tesche, M., Freudenthaler, V., Toledano, C., Wiegner, M., Ansmann, A., Althausen, D., and Seefeldner, M.: Characterization of Saharan dust, marine aerosols and mixtures of biomass burning aerosols and dust by means of multi-wavelength depolarization-and Raman-measurements during SAMUM-2, Tellus B, 63, 706–724, 2011.

Groß, S., Esselborn, M., Weinzierl, B., Wirth, M., Fix, A., and Petzold, A.: Aerosol classification by airborne high spectral resolution lidar observations, Atmos. Chem. Phys., 13, 2487-2505, doi:10.5194/acp-13-2487-2013, 2013.

Groß, S., Freudenthaler, V., Schepanski, K., Toledano, C., Schäfler, A., Ansmann, A. and Weinzierl, B.: Optical properties of long-range transported Saharan dust over Barbados as measured by dual-wavelength depolarization Raman lidar measurements, Atmospheric Chemistry and Physics, 15(19), 11067–11080, doi:10.5194/acp-15-11067-2015, 2015.

Guerrero-Rascado, J. L., Lyamani, H., and Alados-Arboledas, L.: Optical properties of free tropospheric aerosol from multi-wavelength Raman lidars over the southern Iberian Peninsula, in: Proceedings of the 9th International Symposium on Tropospheric Profiling, L'Aquila, Italy, 3–7 September 2012, 2012. 27993.

Guirado, C., Cuevas, E., Cachorro, V. E., Toledano, C., Alonso-Pérez, S., Bustos, J. J., Basart, S., Romero, P. M., Camino, C., Mimouni, M., Zeudmi, L., Goloub, P., Baldasano, J. M., and de Frutos, A. M.: Aerosol characterization at the Saharan AERONET site Tamanrasset, Atmos. Chem. Phys., 14, 11753-11773, doi:10.5194/acp-14-11753-2014, 2014.

Holben, B. N., Eck, T.F., Slutsker, I., Tanre, D., Buis, J.P., Setzer, A., Vermote, E., Reagan, J.A., Kaufman, Y.J., Nakajima, T., Lavenu, F., Jankowiak, I., and Smirnov, A.: AERONET—A Federated Instrument Network and Data Archive for Aerosol Characterization, Remote Sens. Environ. 66, 1–16, doi:10.1016/S0034-4257(98)00031-5, 1998.

Holben, B. N., Tanré, D., Smirnov, A., Eck, T.F., Slutsker, I., Abunhassan, N., Newcomb, W.W., Schafer, J.S., Chatenet, B., Lavenu, F., Kaufman, Y.J., Vande Castle, J., Setzer, A., Markham, B., Clark, D., Frouin, R., Halthore, R., Karneli, A., O'Neill, N.T., Pietras, C., Pinker, R.T., Voss, K., and Zibordi, G.: An emerging ground-based aerosol climatology: Aerosol optical depth from AERONET, J. Geophys. Res., 106(D11), 12067–12097, doi:10.1029/2001JD900014, 2001.

Hsu, N. C., Tsay, S. C., King, M. D. and Herman, J. R.: Aerosol properties over bright-reflecting source regions, IEEE Trans. Geosci. Remote Sens., 42(3), 557-569, doi:10.1109/TGRS.2004.824067, 2004.

Huang, J., Minnis, P., Lin, B., Wang, T., Yi, Y., Hu, Y., Sun-Mack, S., and Ayers, K.: Possible influences of Asian dust aerosols on cloud properties and radiative forcing observed from MODIS and CERES, Geophys. Res. Lett., 33, L06824, doi:10.1029/2005GL024724, 2006.

Huang, J., Guo, J., Wang, F., Liu, Z., Jeong, M.-J., Yu, H., and Zhang, Z.: CALIPSO inferred most probable heights of global dust and smoke layers, J. Geophys. Res., 120(10), 5085-5100, doi:10.1002/2014JD022898, 2015a.

Huang, J. P., Liu, J. J., Chen, B., and Nasiri, S. L.: Detection of anthropogenic dust using CALIPSO lidar measurements, Atmos. Chem. Phys., 15, 11653-11665, doi:10.5194/acp-15-11653-2015, 2015b.

Huneeus, N., Schulz, M., Balkanski, Y., Griesfeller, J., Prospero, J., Kinne, S., Bauer, S., Boucher, O., Chin, M., Dentener, F., Diehl, T., Easter, R., Fillmore, D., Ghan, S., Ginoux, P., Grini, A., Horowitz, L., Koch, D., Krol, M. C., Landing, W., Liu, X., Mahowald, N., Miller, R., Morcrette, J.-J., Myhre, G., Penner, J., Perlwitz, J., Stier, P., Takemura, T., and Zender, C. S.: Global dust model intercomparison in AeroCom phase I, Atmos. Chem. Phys., 11, 7781–7816, doi:10.5194/acp-11-7781-2011, 2011.

Illingworth, A.J., Barker, H.W., Beljaars, A., Ceccaldi, M., Chepfer, H., Clerbaux, N., Cole, J., Delanoë, J., Domenech, C., Donovan, D.P., Fukuda, S., Hirakata, M., Hogan, R.J., Huenerbein, A., Kollias, P., Nakajima, T., Nakajima, T.-Y., Nishizawa, T., Ohno, Y., Okamoto, H., Oki, R., Sato, K., Satoh, M., Sephard, M.W., Velázquez-Blázquez, A., Wandinger, U., Wehr, T., and van Zadelhoff, G.-J.: The EarthCARE Satellite: The Next Step Forward in Global Measurements of Clouds, Aerosols, Precipitation, and Radiation, Bull. Am. Meteorol. Soc., 96, 1311–1332, doi: 10.1175/BAMS-D-12-00227.1,2015.

Ingmann, P., Veihelmann, B., Langen, J., Lamarre, D., Stark, H., and Bazalgette Courrèges-Lacoste, G.: Requirements for the GMES Atmosphere Service and ESA's implementation concept: Sentinels-4/5 and -5p. Remote Sensing of Environment, 120, 58–69. doi:10.1016/j.rse.2012.01.023, 2012.

IPCC 2013: Climate Change 2013: The Physical Science Basis. Contribution of Working Group I to the Fifth Assessment Report of the Intergovernmental Panel on Climate Change, edited by: Stocker, T. F., Qin, D., Plattner, G.-K., Tignor, M., Allen, S. K., Boschung, J., Nauels, A., Xia, Y., Bex, V., and Midgley, P. M., Cambridge University Press, Cambridge, UK and New York, NY, USA, 1535 pp., available at: https://www.ipcc.ch/pdf/assessment-report/ar5/wg1/WG1AR5_Frontmatter_FINAL.pdf (last access: 30 August 2016), 2013.

Israelevich, P. L., Levin, Z., Joseph, J. H., and Ganor, E.: Desert aerosol transport in the Mediterranean region as inferred from the TOMS aerosol index, J. Geophys. Res., 107(D21), 4572, doi:10.1029/2001JD002011, 2002.

Israelevich, P., Ganor, E., Alpert, P., Kishcha, P., and Stupp, A.: Predominant transport paths of Saharan dust over the Mediterranean Sea to Europe, J. Geophys. Res., 117, D02205, doi:10.1029/2011JD016482, 2012.

Kanitz, T., Ansmann, A., Engelmann, R., and Althausen, D.: North-south cross sections of the vertical aerosol distribution over the Atlantic Ocean from multiwavelength Raman/polarization lidar during Polarstern cruises, J. Geophys. Res., 118(6), 2643-2655. doi:10.1002/jgrd.50273, 2013.

Kaufman, Y.J., Remer, L.A., Tanré, D., Li, R.-R., Kleidman, R., Matoo, S., Levy, R., Eck, T., Holben, B.N., Ichoku, C., Martins, V., and Koren, I.: A Critical Examination of the Residual Cloud Contamination and Diurnal Sampling Effects on MODIS Estimates of Aerosol over Ocean, IEEE Transactions on Geoscience and Remote Sensing, 43, 2886–2897. doi:10.1109/TGRS.2005.858430, 2005.

Kinne, S., Schulz, M., Textor, C., Guibert, S., Balkanski, Y., Bauer, S.E., Berntsen, T., Berglen, T., Boucher, O., Chin, M., Collins, W., Dentener, F., Diehl, T., Easter, R., Feichter, H., Fillmore, D., Ghan, S., Ginoux, P., Gong, S., Grini, A., Hendricks, J., Herzog, M., Horrowitz, L., Isaksen, I., Iversen, T., Kirkevg, A., Kloster, S., Koch, D., Kristjansson, J.E., Krol, M., Lauer, A., Lamarque, J.F., Lesins, G., Liu, X., Lohmann, U., Montanaro, V., Myhre, G., Penner, J., Pitari, G., Reddy, S., Seland, O., Stier, P., Takemura, T., and Tie, X.: An AeroCom initial assessment optical properties in aerosol component modules of global models, Atmos. Chem. Phys., 6, 1815-1834, doi:10.5194/acp-6-1815-2006, 2006.

Koren, I., Feingold, G., and Remer, L. A.: The invigoration of deep convective clouds over the Atlantic: aerosol effect, meteorology or retrieval artifact?, Atmos. Chem. Phys., 10, 8855–8872, doi:10.5194/acp-10-8855-2010, 2010.

Kosmopoulos, P. G., Kaskaoutis, D. G., Nastos, P. T., and Kambezidis, H. D.: Seasonal variation of columnar aerosol optical properties over Athens, Greece, based on MODIS data, Remote Sens. Environ., 112, 2354-2366, doi:10.1016/j.rse.2007.11.006, 2008.

Lelieveld, J., Berresheim, H., Borrmann, S., Crutzen, P.J., Dentener, F.J., Fischer, H., Feichter, J., Flatau, P.J., Heland, J., Holzinger, R., Korrmann, R., Lawrence, M.G., Levin, Z., Markowicz, K.M., Mihalopoulos, N., Minikin, A., Ramanathan, V., de Reus, M., Roelofs, G.J., Scheeren, H.A., Sciare, J., Schlanger, H., Schultz, M., Siegmund, P., Steil, B., Stephanou, E.G., Stier, P., Traub, M., Warneke, C., Williams, J., and Ziereis, H.: Global Air Pollution Crossroads over the Mediterranean, Science, 298, 794–799. doi:10.1126/science.1075457, 2002.

Levin, Z., Teller, A., Ganor, E., and Yin, Y.: On the interactions of mineral dust, sea-salt particles, and clouds: A measurement and modeling study from the Mediterranean Israeli Dust Experiment campaign, J. Geophys. Res., 110, D20202, doi:10.1029/2005JD005810, 2005.

Li, F., Vogelmann, A.M., and Ramanathan, V.: Saharan Dust Aerosol Radiative Forcing Measured from Space, J. Climate, 17, 2558–2571, doi: 10.1175/1520-0442(2004)017<2558:SDARFM>2.0.CO;2, 2004.

Li, J., Carlson, B. E., and Lacis, A. A.: Application of spectral analysis techniques to the intercomparison of aerosol data – Part 4: Synthesized analysis of multisensor satellite and ground-based AOD measurements using combined maximum covariance analysis, Atmos. Meas. Tech., 7, 2531-2549, doi:10.5194/amt-7-2531-2014, 2014.

Liu, Z., Sugimoto, N. and Murayama, T.: Extinction-to-backscatter ratio of Asian dust observed with high-spectral-resolution lidar and Raman lidar, Applied Optics, 41(15), 2760, doi:10.1364/AO.41.002760, 2002.

Liu, D., Wang, Z., Liu, Z., Winker, D., and Trepte, C.:A height resolved global view of dust aerosols from the first year CALIPSO lidar measurements, J. Geophys. Res., 113, D16214, doi:10.1029/2007JD009776, 2008a.

Liu, Z., Omar, A., Vaughan, M., Hair, J., Kittaka, C., Hu, Y., Powell, K., Trepte, C., Winker, D., Hostetler, C., Ferrare, R., and Pierce, R.: CALIPSO lidar observations of the optical properties of Saharan dust: A case study of long-range transport, J. Geophys. Res., 113, D07207, doi:10.1029/2007JD008878, 2008b.

Maheras, P., Flocas, H.A., Patrikas, I. and Anagnostopoulou, C.: A 40 year objective climatology of surface cyclones in the Mediterranean region: spatial and temporal distribution, Int. J. Climatol., 21, 109–130. doi:10.1002/joc.599, 2001.

Mallet, M., Tulet, P., Serça, D., Solmon, F., Dubovik, O., Pelon, J., Pont, V., and Thouron, O.: Impact of dust aerosols on the radiative budget, surface heat fluxes, heating rate profiles and convective activity over West Africa during March 2006, Atmos. Chem. Phys., 9, 7143-7160, doi:10.5194/acp-9-7143-2009, 2009.

Mamouri, R. E., Amiridis, V., Papayannis, A., Giannakaki, E., Tsaknakis, G., and Balis, D. S.: Validation of CALIPSO space-borne-derived attenuated backscatter coefficient profiles using a ground-based lidar in Athens, Greece, Atmos. Meas. Tech., 2, 513-522, doi:10.5194/amt-2-513-2009, 2009.

Mamouri, R. E., and Ansmann, A.: Fine and coarse dust separation with polarization lidar, Atm. Meas. Tech., 7(11), 3717–3735, doi:10.5194/amt-7-3717-2014, 2014.

Mamouri, R. E., and Ansmann, A.: Estimated desert-dust ice nuclei profiles from polarization lidar: methodology and case studies, Atmos. Chem. Phys., 15, 3463-3477, doi:10.5194/acp-15-3463-2015, 2015.

Mamouri, R.-E. and Ansmann, A.: Potential of polarization lidar to provide profiles of CCN- and INP-relevant aerosol parameters, Atmos. Chem. Phys., 16, 5905-5931, doi:10.5194/acp-16-5905-2016, 2016.

Mamouri, R. E., and Ansmann, A.: Fine and coarse dust separation with polarization lidar: Extended methodology for multiple wavelengths, to be submitted to AMT SALTRACE Special Issue.

Marey, H. S., Gille, J. C., El-Askary, H. M., Shalaby, E. A., and El-Raey, M. E.: Aerosol climatology over Nile Delta based on MODIS, MISR and OMI satellite data, Atmos. Chem. Phys., 11, 10637-10648, doi:10.5194/acp-11-10637-2011, 2011.

Mariotti, A., Struglia, M.V., Zeng, N., and Lau, K.-M.: The Hydrological Cycle in the Mediterranean Region and Implications for the Water Budget of the Mediterranean Sea, Journal of Climate, 15, 1674–1690, doi:10.1175/1520-0442(2002)015<1674:THCITM>2.0.CO;2, 2002.

Mona, L., Amodeo, A., Pandolfi, M., and Pappalardo, G.: Saharan dust intrusions in the Mediterranean area: three years of Ra-man lidar measurements, J. Geophys. Res.-Atmos., 111, d16203, doi:10.1029/2005JD006569, 2006.

Mona, L., Liu, Z., Müller, D., Omar, A., Papayannis, A., Sugimoto, N., Pappalardo, G., and Vaughan, M.: Lidar Measurements for Desert Dust Characterization: An Overview, Adv. Meteorol., 2012, pp. 36, doi:10.1155/2012/356265, 2012.

Mona, L., Papagiannopoulos, N., Basart, S., Baldasano, J., Binietoglou, I., Cornacchia, C., and Pappalardo, G.: EARLINET dust observations vs. BSC-DREAM8b modeled profiles: 12-year-long systematic comparison at Potenza, Italy, Atmos. Chem. Phys., 14, 8781-8793, doi:10.5194/acp-14-8781-2014, 2014.

Moulin, C, Lambert, C.E., Dayan, U., Masson, V., Ramonet, M., Bousquet, P., Legrand, M., Balkanski, Y.J., Guelle, W., Marticorena, B., Bergametti, F., and Dulac, F.: Satellite climatology of African dust transport in the Mediterranean atmosphere, J. Geophys. Res., 103(D11), 13137–13144, doi:10.1029/98JD00171, 1998.

Müller, D., Mattis, I., Wandinger, U., Ansmann, A., Althausen, D., Dubovik, O., Eckhardt, S., and Stohl, A.: Saharan dust over a central European EARLINET-AERONET site: Combined observations with Raman lidar and Sun photometer, J. Geophys. Res., 108, 4345, doi:10.1029/2002JD002918, 2003.

Nabat, P., Solmon, F., Mallet, M., Kok, J. F., and Somot, S.: Dust emission size distribution impact on aerosol budget and radiative forcing over the Mediterranean region: a regional climate model approach, Atmos. Chem. Phys., 12, 10545-10567, doi:10.5194/acp-12-10545-2012, 2012.

Nabat, P., Somot, S., Mallet, M., Chiapello, I., Morcrette, J. J., Solmon, F., Szopa, S., Dulac, F., Collins, W., Ghan, S., Horowitz, L. W., Lamarque, J. F., Lee, Y. H., Naik, V., Nagashima, T., Shindell, D., and Skeie, R.: A 4-D climatology (1979-2009) of the monthly tropospheric aerosol optical depth distribution over the Mediterranean region from a comparative evaluation and blending of remote sensing and model products, Atmos. Meas. Tech., 6, 1287-1314, doi:10.5194/amt-6-1287-2013, 2013.

O'Neill, N. T., Eck, T. F., Smirnov, A., Holben, B. N. and Thulasiraman, S.: Spectral discrimination of coarse and fine mode optical depth, J. Geophys. Res., 108(D17), 4559, doi:10.1029/2002JD002975, 2003

Omar, A., Winker, D., Kittaka, C., Vaughan, M., Liu, Z., Hu, Y. X., Trepte, C., Rogers, R., Ferrare, R., Lee, K., Kuehn, R., and Hostetler, C.: The CALIPSO automated aerosol classification and lidar ratio selection algorithm, J. Atmos. Ocean. Tech., 26, 1994–2014, doi:10.1175/2009jtecha1231.1, 2009.

Omar, A. H., Winker, D. M., Tackett, J. L., Giles, D. M., Kar, J., Liu, Z., Vaughan, M. A., Powell, K. A., and Trepte, C. R.: CALIOP and AERONET aerosol optical depth comparisons: one size fits none, J. Geophys. Res.-Atmos., 118, 4748–4766, doi:10.1002/jgrd.50330, 2013.

Papadimas, C. D., Hatzianastassiou, N., Mihalopoulos, N., Querol, X., and Vardavas, I.: Spatial and temporal variability in aerosol properties over the Mediterranean basin based on 6-year (2000-2006) MODIS data, J. Geophys. Res., 113(D11), D11205, doi:10.1029/2007JD009189, 2008.

Papagiannopoulos, N., Mona, L., Alados-Arboledas, L., Amiridis, V., Baars, H., Binietoglou, I., Bortoli, D., D'Amico, G., Giunta, A., Guerrero-Rascado, J. L., Schwarz, A., Pereira, S., Spinelli, N., Wandinger, U., Wang, X., and Pappalardo, G.: CALIPSO climatological products: evaluation and suggestions from EARLINET, Atmos. Chem. Phys., 16, 2341-2357, doi:10.5194/acp-16-2341-2016, 2016.

Papayannis, A., Balis, D., Amiridis, V., Chourdakis, G., Tsaknakis, G., Zerefos, C., Castanho, A. D. A., Nickovic, S., Kazadzis, S., and Grabowski, J.: Measurements of Saharan dust aerosols over the Eastern Mediterranean using elastic backscatter-Raman lidar, spectrophotometric and satellite observations in the frame of the EARLINET project, Atmos. Chem. Phys., 5, 2065-2079, doi:10.5194/acp-5-2065-2005, 2005.

Papayannis, A., Amiridis, V., Mona, L., Tsaknakis, G., Balis, D., Bösenberg, J., Chaikovski, A., De Tomasi, F., Grigorov, I., Mat-tis, I., Mitev, V., Müller, D., Nickovic, S., Pérez, C., Pietruczuk, A., Pisani, G., Ravetta, F., Rizi, V., Sicard, M., Trickl, T., Wiegner, M., Gerding, M., Mamouri, R. E., D'Amico, G., and Pappalardo, G.: Systematic lidar observations of Saharan dust over Europe in the frame of EARLINET (2000–2002), J. Geophys. Res., 113, D10204, doi:10.1029/2007JD009028, 2008.

Pappalardo, G., Amodeo, A., Pandolfi, M., Wandinger, U., Ansmann, A., Bösenberg, J., Matthias, V., Amiridis, V., De Tomasi, F., Frioud, M., Iarlori, M., Komguem, L., Papayannis, A., Rocadenbosch, F., and Wang, X.: Aerosol lidar

intercomparison in the framework of the EARLINET project. 3. Raman lidar algorithm for aerosol extinction, backscatter, and lidar ratio, Appl. Opt., 43, 5370-5385, doi:10.1364/AO.43.005370, 2004.

Pappalardo, G., Wandinger, U., Mona, L., Hiebsch, A., Mattis, I., Amodeo, A., Ansmann, A., Seifert, P., Linné, H., Apituley, A., Alados Arboledas, L., Balis, D., Chaikovsky, A., D'Amico, G., De Tomasi, F., Freudenthaler, V., Giannakaki, E., Giunta, A., Grigorov, I., Iarlori, M., Madonna, F., Mamouri, R., Nasti, L., Papayannis, A., Pietruczuk, A., Pujadas, M., Rizi, V., Roca-denbosch, F., Russo, F., Schnell, F., Spinelli, N., Wang, X., and Wiegner, M.: EARLINET correlative measurements for CALIPSO: first intercomparison results, J. Geophys. Res., 115, D00H19, doi:10.1029/2009JD012147, 2010.

Pey, J., Querol, X., Alastuey, A., Forastiere, F., and Stafoggia, M.: African dust outbreaks over the Mediterranean Basin during 2001–2011: PM_{10} concentrations, phenomenology and trends, and its relation with synoptic and mesoscale meteorology, Atmos. Chem. Phys., 13, 1395-1410, doi:10.5194/acp-13-1395-2013, 2013.

Popp, T., de Leeuw, G., Bingen, C., Brühl, C., Capelle, V., Chedin, A., Clarisse, L., Dubovik, O., Grainger, R., Griesfeller, J., Heckel, A., Kinne, S., Klüser, L., Kosmale, M., Kolmonen, P., Lelli, L., Litvinov, P., Mei, L., North, P., Pinnock, S., Povey, A., Robert, C., Schulz, M., Sogacheva, L., Stebel, K., Stein Zweers, D., Thomas, G., Tilstra, L.G., Vandenbussche, S., Veefkind, P., Vountas, M., and Xue, Y.: Development, Production and Evaluation of Aerosol Climate Data Records from European Satellite Observations (Aerosol_cci). Remote Sens., 8(5), 421, doi:10.3390/rs8050421, 2016.

Preißler, J., Bravo-Aranda, J.A., Wagner, F., Granados-Muñoz, M.J., Navas-Guzmán, F., Guerrero-Rascado, J.L., Lyamani, H., and Alados-Arboledas, L.: Combined observations with multi-wavelength Raman lidars and sun photometers on the southern Iberian Peninsula, European Aerosol Conference 2012, Granada, Spain, 2012.

Prospero, J. M.: Long-term measurements of the transport of African mineral dust to the southeastern United States: Implications for regional air quality, J. Geophys. Res., 104(D13), 15917–15927, doi:10.1029/1999JD900072, 1999.

Prospero, J. M., Ginoux, P., Torres, O., Nicholson, S.E., and Gill, T.E.: Environmental Characterization of Global Sources of Atmospheric Soil Dust Identified with the NIMBUS 7 Total Ozone Mapping Spectrometer (TOMS) Absorbing Aerosol Product, Rev. Geophys., 40(1), 1002, doi:doi:10.1029/2000RG000095, 2002.

Prospero, J. M., and Lamb, P.J.: African Droughts and Dust Transport to the Caribbean: Climate Change Implications, Science, 302, 1024–1027, doi:10.1126/science.1089915, 2003.

Ridley, D. A., Heald, C. L., and Ford, B.: North African dust export and deposition: A satellite and model perspective, J. Geophys. Res., 117, D02202, doi:10.1029/2011JD016794, 2012.

Rosenfeld, D., Rudich, Y.. and Lahav, R.: Desert Dust Suppressing Precipitation: A Possible Desertification Feedback Loop, Proceedings of the National Academy of Sciences, 98, 5975–5980, doi: 10.1073/pnas.101122798, 2001.

Sakai, T., Shibata, T., Kwon, S-A., Kim, Y.-S., Tamura, K., and Iwasaka Y.: Free tropospheric aerosol backscatter, depolarization ratio, and relative humidity measured with the Raman lidar at Nagoya in 1994–1997: contributions of

aerosols from the Asian continent and the pacific ocean, Atmos Environ, 34, 431–442, doi:10.1016/S1352-2310(99)00328-3, 2000.

Sanders, A. F. J., de Haan, J. F., Sneep, M., Apituley, A., Stammes, P., Vieitez, M. O., Tilstra, L. G., Tuinder, O. N. E., Koning, C. E., and Veefkind, J. P.: Evaluation of the operational Aerosol Layer Height retrieval algorithm for Sentinel-5 Precursor: application to O2 A band observations from GOME-2A, Atmos. Meas. Tech., 8, 4947-4977, doi:10.5194/amt-8-4947-2015, 2015.

Sayer, A. M., Hsu, N. C., Bettenhausen, C., and Jeong, M. J.: Validation and uncertainty estimates for MODIS Collection 6 "deep Blue" aerosol data, J. Geophys. Res. Atmos., 118(14), 7864-7872, doi:10.1002/jgrd.50600, 2013.

Schepanski, K., Tegen, I., Laurent, B., Heinold, B., and Macke, A.: A new Saharan dust source activation frequency map derived from MSG-SEVIRI IR-channels, Geophys. Res. Lett., 34, L18803, doi:10.1029/2007GL030168, 2007.

Schepanski, K., Tegen, I., Todd, M.C., Heinold, B., Bönisch, G., Laurent, B., and Macke, A.: Meteorological processes forcing Saharan dust emission inferred from MSG-SEVIRI observations of subdaily dust source activation and numerical models, J. Geophys. Res., 114, D10201, doi:10.1029/2008JD010325, 2009.

Schuster, G. L., Vaughan, M., MacDonnell, D., Su, W., Winker, D., Dubovik, O., Lapyonok, T., and Trepte, C.: Comparison of CALIPSO aerosol optical depth retrievals to AERONET mea-surements, and a climatology for the lidar ratio of dust, Atmos. Chem. Phys., 12, 7431–7452, doi:10.5194/acp-12-7431-2012, 2012.

Shahgedanova, M., Kutuzov, S., White, K., and Nosenko, G.: Using the significant dust deposition event on the glaciers of Mt. Elbrus, Caucasus Mountains, Russia on 5 May 2009 to develop a method for dating and provenancing of desert dust events recorded in snow pack, Atmos. Chem. Phys., 13, 1797–1808, 2013, doi:10.5194/acp-13-1797-2013, 2013

Solomon, S., Plattner, G.-K., Knutti, R., and Friedlingstein P.: Irreversible Climate Change due to Carbon Dioxide Emissions, Proceedings of the National Academy of Sciences, 106, 1704–1709, doi:10.1073/pnas.0812721106, 2009.

Steinke, I., Hoose, C., Möhler, O., Connolly, P., and Leisner, T.: A new temperature- and humidity-dependent surface site density approach for deposition ice nucleation, Atmos. Chem. Phys., 15, 3703–3717, doi:10.5194/acp-15-3703-2015, 2015.

Su, W. et al: Global all-sky shortwave direct radiative forcing of anthropogenic aerosols from combined satellite observations and GOCART simulations. J. Geoph. Res. D: Atmospheres, 118(2), 655-669, 2013.

Tegen, I., Hollrig, P., Chin, M., Fung, I., Jacob, D., and Penner, J.: Contribution of different aerosol species to the global aerosol extinction optical thickness: Estimates from model results, J. Geophys. Res., 102, 23895-23915, doi:10.1029/97JD01864, 1997.

Tesche, M., Ansmann, A., Müller, D., Althausen, D., Engelmann, R., Freudenthaler, V., and Grob, S.: Vertically Resolved Separation of Dust and Smoke over Cape Verde Using Multiwavelength Raman and Polarization Lidars during Saharan Mineral Dust Experiment 2008, J. Geophys. Res., 114, D13202, doi:10.1029/2009JD011862, 2009.

Tesche, M., Wandinger, U., Ansmann, A., Althausen, D., Müller, D., and Omar, A. H.: Ground-based validation of CALIPSO observations of dust and smoke in the Cape Verde region, J. Geophys. Res. Atmos., 118, 2889–2902–, doi:10.1002/jgrd.50248, 2013.

Textor, C., Schulz, M., Guibert, S., Kinne, S., Balkanski, Y., Bauer, S., Berntsen, T., Berglen, T., Boucher, O., Chin, M., Dentener, F., Diehl, T., Easter, R., Feichter, H., Fillmore, D., Ghan, S., Ginoux, P., Gong, S., Grini, A., Hendricks, J., Horowitz, L., Huang, P., Isaksen, I., Iversen, I., Kloster, S., Koch, D., Kirkevag, A., Kristjansson, J. E., Krol, M., Lauer, A., Lamarque, J. F., Liu, X., Montanaro, V., Myhre, G., Penner, J., Pitari, G., Reddy, S., Seland, Ø., Stier, P., Takemura, T., and Tie, X.: Analysis and quantification of the diversities of aerosol life cycles within AeroCom, Atmos. Chem. Phys., 6, 1777–1813, doi:10.5194/acp-6-1777-2006, 2006.

The EARLINET publishing group 2000–2010: Adam, M., Alados-Arboledas, L., Al-thausen, D., Amiridis, V., Amodeo, A., Ansmann, A., Apituley, A., Arshinov, Y., Balis, D., Belegante, L., Bobrovnikov, S., Boselli, A., Bravo-Aranda, J. A., Bösen-berg, J., Carstea, E., Chaikovsky, A., Comerón, A., D'Amico, G., Daou, D., Dreischuh, T., Engelmann, R., Finger, F., Freudenthaler, V., Garcia-Vizcaino, D., García, A. J. F., Geiß, A., Giannakaki, E., Giehl, H., Giunta, A., de Graaf, M., Grana-dos-Muñoz, M. J., Grein, M., Grigorov, I., Groß, S., Gruening, C., Guerrero-Rascado, J. L., Haeffelin, M., Hayek, T., Iarlori, M., Kanitz, T., Kokkalis, P., Linné, H., Ma-donna, F., Mamouriat, R.-E., Matthias, V., Mattis, I., Menéndez, F. M., Mitev, V., Mona, L., Morille, Y., Muñoz, C., Müller, A., Müller, D., Navas-Guzmán, F., Nemuc, A., Nicolae, D., Pandolfi, M., Papayannis, A., Pappalardo, G., Pelon, J., Perrone, M. R., Pietruczuk, A., Pisani, G., Potma, C., Preißler, J., Pujadas, M., Putaud, J., Radu, C., Ravetta, F., Reigert, A., Rizi, V., Rocadenbosch, F., Rodríguez, A., Sauvage, L., Schmidt, J., Schnell, F., Schwarz, A., Seifert, P., Serikov, I., Sicard, M., Silva, A. M., Simeonov, V., Siomos, N., Sirch, T., Spinelli, N., Stoyanov, D., Talianu, C., Tesche, M., De Tomasi, F., Trickl, T., Vaughan, G., Volten, H., Wagner, F., Wandinger, U., Wang, X., Wiegner, M., and Wilson, K. M.: EARLINET all observations (2000–2010), World Data Center for Climate (WDCC), doi:10.1594/WDCC/EN_all_measurements_2000-2010, 2014a.

The EARLINET publishing group 2000–2010: Adam, M., Alados-Arboledas, L., Al-thausen, D., Amiridis, V., Amodeo, A., Ansmann, A., Apituley, A., Arshinov, Y., Balis, D., Belegante, L., Bobrovnikov, S., Boselli, A., Bravo-Aranda, J. A., Bösen-berg, J., Carstea, E., Chaikovsky, A., Comerón, A., D'Amico, G., Daou, D., Dreischuh, T., Engelmann, R., Finger, F., Freudenthaler, V., Garcia-Vizcaino, D., García, A. J. F., Geiß, A., Giannakaki, E., Giehl, H., Giunta, A., de Graaf, M., Grana-dos-Muñoz, M. J., Grein, M., Grigorov, I., Groß, S., Gruening, C., Guerrero-Rascado, J. L., Haeffelin, M., Hayek, T., Iarlori, M., Kanitz, T., Kokkalis, P., Linné, H., Ma-donna, F., Mamouriat, R.E., Matthias, V., Mattis, I., Menéndez, F. M., Mitev, V., Mona, L., Morille, Y., Muñoz, C., Müller, A., Müller, D., Navas-Guzmán, F., Nemuc, A., Nicolae, D., Pandolfi, M., Papayannis, A., Pappalardo, G., Pelon, J., Perrone, M.R., Pietruczuk, A., Pisani, G., Potma, C., Preißler, J., Pujadas, M., Putaud, J., Radu, C., Ravetta, F., Reigert, A., Rizi, V., Rocadenbosch, F., Rodríguez, A., Sauvage, L., Schmidt, J., Schnell, F., Schwarz, A., Seifert, P., Serikov, I., Sicard, M., Silva, A. M., Simeonov, V., Siomos, N., Sirch, T., Spinelli, N., Stoyanov, D., Talianu, C., Tesche, M., De Tomasi, F., Trickl, T., Vaughan, G., Volten, H., Wagner, F.,

Wandinger, U., Wang, X., Wiegner, M., and Wilson, K. M.: EARLINET climatology (2000–2010), World Data Center for Climate (WDCC), doi:10.1594/WDCC/EN_Climatology_2000-2010, 2014b.

The EARLINET publishing group 2000–2010: Adam, M., Alados-Arboledas, L., Al-thausen, D., Amiridis, V., Amodeo, A., Ansmann, A., Apituley, A., Arshinov, Y., Balis, D., Belegante, L., Bobrovnikov, S., Boselli, A., Bravo-Aranda, J. A., Bösen-berg, J., Carstea, E., Chaikovsky, A., Comerón, A., D'Amico, G., Daou, D., Dreischuh, T., Engelmann, R., Finger, F., Freudenthaler, V., Garcia-Vizcaino, D., García, A. J. F., Geiß, A., Giannakaki, E., Giehl, H., Giunta, A., de Graaf, M., Grana-dos-Muñoz, M. J., Grein, M., Grigorov, I., Groß, S., Gruening, C., Guerrero-Rascado, J. L., Haeffelin, M., Hayek, T., Iarlori, M., Kanitz, T., Kokkalis, P., Linné, H., Ma-donna, F., Mamouriat, R.-E., Matthias, V., Mattis, I., Menéndez, F. M., Mitev, V., Mona, L., Morille, Y., Muñoz, C., Müller, A., Müller, D., Navas-Guzmán, F., Nemuc, A., Nicolae, D., Pandolfi, M., Papayannis, A., Pappalardo, G., Pelon, J., Perrone, M. R., Pietruczuk, A., Pisani, G., Potma, C., Preißler, J., Pujadas, M., Putaud, J., Radu, C., Ravetta, F., Reigert, A., Rizi, V., Rocadenbosch, F., Rodríguez, A., Sauvage, L., Schmidt, J., Schnell, F., Schwarz, A., Seifert, P., Serikov, I., Sicard, M., Silva, A. M., Simeonov, V., Siomos, N., Sirch, T., Spinelli, N., Stoyanov, D., Talianu, C., Tesche, M., De Tomasi, F., Trickl, T., Vaughan, G., Volten, H., Wagner, F., Wandinger, U., Wang, X., Wiegner, M., and Wilson, K. M.: EARLINET correlative observations for CALIPSO (2006–2010),World Data Center for Climate (WDCC), doi:10.1594/WDCC/EN_Calipso_2006-2010, 2014c.

The EARLINET publishing group 2000-2010, Adam, M., Alados-Arboledas, L., Al-thausen, D., Amiridis, V., Amodeo, A., Ansmann, A., Apituley, A., Arshinov, Y., Balis, D., Belegante, L., Bobrovnikov, S., Boselli, A., Bravo-Aranda, J. A., Bösen-berg, J., Carstea, E., Chaikovsky, A., Comerón, A., D'Amico, G., Daou, D., Dreischuh, T., Engelmann, R., Finger, F., Freudenthaler, V., Garcia-Vizcaino, D., García, A. J. F., Geiß, A., Giannakaki, E., Giehl, H., Giunta, A., de Graaf, M., Grana-dos-Muñoz, M. J., Grein, M., Grigorov, I., Groß, S., Gruening, C., Guerrero-Rascado, J. L., Haeffelin, M., Hayek, T., Iarlori, M., Kanitz, T., Kokkalis, P., Linné, H., Ma-donna, F., Mamouriat, R.-E., Matthias, V., Mattis, I., Menéndez, F. M., Mitev, V., Mona, L., Morille, Y., Muñoz, C., Müller, A., Müller, D., Navas-Guzmán, F., Nemuc, A., Nicolae, D., Pandolfi, M., Papayannis, A., Pappalardo, G., Pelon, J., Perrone, M. R., Pietruczuk, A., Pisani, G., Potma, C., Preißler, J., Pujadas, M., Putaud, J., Radu, C., Ravetta, F., Reigert, A., Rizi, V., Rocadenbosch, F., Rodríguez, A., Sauvage, L., Schmidt, J., Schnell, F., Schwarz, A., Seifert, P., Serikov, I., Sicard, M., Silva, A. M., Simeonov, V., Siomos, N., Sirch, T., Spinelli, N., Stoyanov, D., Talianu, C., Tesche, M., De Tomasi, F., Trickl, T., Vaughan, G., Volten, H., Wagner, F., Wandinger, U., Wang, X., Wiegner, M., and Wilson, K. M.: EARLINET observations related to vol-canic eruptions (2000–2010), World Data Center for Climate (WDCC), doi:10.1594/WDCC/EN_VolcanicEruption_2000-2010, 2014d.

The EARLINET publishing group 2000–2010: Adam, M., Alados-Arboledas, L., Al-thausen, D., Amiridis, V., Amodeo, A., Ansmann, A., Apituley, A., Arshinov, Y., Balis, D., Belegante, L., Bobrovnikov, S., Boselli, A., Bravo-Aranda, J. A., Bösen-berg, J., Carstea, E., Chaikovsky, A., Comerón, A., D'Amico, G., Daou, D., Dreischuh, T., Engelmann, R., Finger, F., Freudenthaler, V., Garcia-Vizcaino, D., García, A. J. F., Geiß, A., Giannakaki, E., Giehl, H., Giunta, A., de Graaf, M., Grana-dos-Muñoz, M. J., Grein, M., Grigorov, I., Groß, S., Gruening, C., Guerrero-Rascado, J. L., Haeffelin, M., Hayek, T., Iarlori, M., Kanitz, T., Kokkalis, P., Linné, H., Ma-donna, F., Mamouriat, R.-E., Matthias, V., Mattis, I., Menéndez,

F. M., Mitev, V., Mona, L., Morille, Y., Muñoz, C., Müller, A., Müller, D., Navas-Guzmán, F., Nemuc, A., Nicolae, D., Pandolfi, M., Papayannis, A., Pappalardo, G., Pelon, J., Perrone, M. R., Pietruczuk, A., Pisani, G., Potma, C., Preißler, J., Pujadas, M., Putaud, J., Radu, C., Ravetta, F., Reigert, A., Rizi, V., Rocadenbosch, F., Rodríguez, A., Sauvage, L., Schmidt, J., Schnell, F., Schwarz, A., Seifert, P., Serikov, I., Sicard, M., Silva, A. M., Simeonov, V., Siomos, N., Sirch, T., Spinelli, N., Stoyanov, D., Talianu, C., Tesche, M., De Tomasi, F., Trickl, T., Vaughan, G., Volten, H., Wagner, F., Wandinger, U., Wang, X., Wiegner, M., and Wilson, K. M.: EARLINET observations related to Sa-haran Dust events (2000–2010), World Data Center for Climate (WDCC), doi:10.1594/WDCC/EARLINET_SaharanDust_2000-2010, 2014e.

Toledano, C., Wiegner, M., Gross, S., Freudenthaler, V., Gasteiger, J., Müller, D., Müller, T., Schladitz, A., Weinzierl, B., Torres B., and O'Neill, N. T.: Optical properties of aero-sol mixtures derived from sun-sky radiometry during SAMUM-2. Tellus 63B, 635-648, doi: 10.1111/j.1600-0889.2011.00573.x, 2011.Trigo, I.F., Davies, T.D., and Bigg, G.R: Objective climatology of cyclones in the Mediterranean region, Journal of Climate 12, 1685–1696, doi:10.1175/1520-0442(1999)012<1685:OCOCIT>2.0.CO;2, 1999.

Tsamalis, C., Chédin, A., Pelon, J., and Capelle, V.: The seasonal vertical distribution of the Saharan Air Layer and its modulation by the wind, Atmos. Chem. Phys., 13, 11235-11257, doi:10.5194/acp-13-11235-2013, 2013.

Tsikerdekis, A., Zanis, P., Steiner, A. L., Solmon, F., Amiridis, V., Marinou, E., Katragkou, E., Karacostas, T., and Foret, G.: Dust size parameterization in RegCM4: Impact on aerosol burden and radiative forcing, Atmos. Chem. Phys. Discuss., doi:10.5194/acp-2016-434, in review, 2016.

Vaughan, M. A., Powell, K. A., Kuehn, R. E., Young, S. A., Winker, D. M., Hostetler, C. A., Hunt, W. H., Liu, Z., Mcgill, M. J., and Getzewich, B. J.: Fully automated detection of cloud and aerosol layers in the CALIPSO lidar measurements, Journal of Atmospheric and Oceanic Technology, 26 (10), pp. 2034-2050, doi:10.1175/2009JTECHA1228.1, 2009.

Veselovskii, I., Goloub, P., Podvin, T., Bovchaliuk, V., Derimian, Y., Augustin, P., Fourmentin, M., Tanre, D., Korenskiy, M., Whiteman, D. N., Diallo, A., Ndiaye, T., Kolgotin, A., and Dubovik, O.: Retrieval of optical and physical properties of African dust from multiwavelength Raman lidar measurements during the SHADOW campaign in Senegal, Atmos. Chem. Phys., 16, 7013-7028, doi:10.5194/acp-16-7013-2016, 2016.

Viana, M., Querol, X., Alastuey, A., Cuevas, E., and Rodríguez, S.:Influence of African dust on the levels of atmospheric particulates in the Canary Islands air quality network, Atmos. Environ., 36, 5861–5875, doi:10.1016/S1352-2310(02)00463-6, 2002.

Wandinger, U., Tesche, M., Seifert, P., Ansmann, A., Müller, D., and Althausen, D.: Size matters: Influence of multiple scattering on CALIPSO light-extinction profiling in desert dust, Geophys. Res. Lett., 37, L10801, doi:10.1029/2010GL042815, 2010.

Winker, D. M., Vaughan, M. A., Omar, A. H., Hu, Y., Powell, K. A., Liu, Z., Hunt, W. H., and Young, S. A.: Overview of the CALIPSO Mission and CALIOP Data Processing Algorithms, J. Atmos. Oceanic Technol., vol 26, pp. 2310–2323, doi: 10.1175/2009JTECHA1281.1, 2009.

Winker, D. M., Tackett, J. L., Getzewich, B. J., Liu, Z., Vaughan, M. A., and Rogers, R. R.: The global 3-D distribution of tropospheric aerosols as characterized by CALIOP, Atmos. Chem. Phys., 13, 3345–3361, doi:10.5194/acp-13-3345-2013, 2013.

Yang, W., Marshak, A., Várnai, T., Kalashnikova, O. V., and Kostinski, A. B.: CALIPSO observations of transatlantic dust: vertical stratification and effect of clouds, Atmos. Chem. Phys., 12, 11339-11354, doi:10.5194/acp-12-11339-2012, 2012.

Yorks, J. E., McGill, M., Rodier, S., Vaughan, M., Hu, Y., and Hlavka, D.: Radiative effects of African dust and smoke observed from Clouds and the Earth's Radiant Energy System (CERES) and Cloud-Aerosol Lidar with Orthogonal Polarization (CALIOP) data, J. Geophys. Res., 114, D00H04, doi:10.1029/2009JD012000, 2009.

Young, S. and Vaughan, M.: The retrieval of profiles of particulate extinction from Cloud Aerosol Lidar Infrared Pathfinder Satellite, Observations (CALIPSO) data: algorithm description, J. Atmos. Ocean. Tech., 26, 1105–1119, doi:http://dx.doi.org/10.1175/2008JTECHA1221.1, 2009.

Zanis, P., Maillard, E., Stahelin, J., Zerefos, C., Kosmidis, E., and Tourpali, K.: On the turnaround of stratospheric ozone trends deduced from the re-evaluated Umkehr record of Arosa, Switzerland, Journal of Geophysical Research, 111, D22307, doi:10.1029/2005JD006886, 2006.

Zender, C.S., Miller, R.L., and Tegen, I. : Quantifying mineral dust mass budgets: Terminology, constraints, and current estimates. Eos Trans. Amer. Geophys. Union, 85, no. 48, 509, 512, 2004.

Zhang, J., and Christopher, S.A.: Longwave radiative forcing of Saharan dust aerosols estimated from MODIS, MISR, and CERES observations on Terra, Geophys. Res. Lett., 30, 2188, doi:10.1029/2003GL018479, 2003.

Zhang, J. and Reid, J. S.: A decadal regional and global trend analysis of the aerosol optical depth using a data-assimilation grade over-water MODIS and Level 2 MISR aerosol products, Atmos. Chem. Phys., 10, 10949-10963, doi:10.5194/acp-10-10949-2010, 2010.

Atmos. Chem. Phys. Discuss., doi:10.5194/acp-2016-902, 2016
Manuscript under review for journal Atmos. Chem. Phys.
Published: 24 November 2016

Atmospheric Chemistry and Physics Discussions

Tables and Figures

Figure 1: Geographical distribution of the seasonal dust occurrences (a ,c ,e ,d) and the mean AOD values (b ,d ,f ,h) for the three-month averages: January–March (a ,b), April-June (c ,d), July–September (e ,f), and October–November (g ,h), and the domain between 20° W-30° E and 20°-60° N for the period 2007-2015, measured with the CALIPSO climatological dust product.

Figure 2: Geographical distribution of the dust top height (a-d) and the center of mass (e-h) in km a.s.e. measured with CALIPSO dust product for the three-month averages: January–March (a, e), April-June (b, f), July–September (c, g), and October–November (d, h), and the domain between 20° W-30° E and 20°-60° N for the period 2007-2015.

Figure 3: Geographical zonal distribution of the climatological dust extinction coefficient values (Mm^{-1}) measured by CALIPSO dust product for the regions 10° W to 20° W (a-d), 0° to 10° W (e-h), 0° to 10° E (i-l), 10° E to 20° E (m-p), and 20° E to 30° E (q-t) for the latitudinal regions from 10° N-60° N as illustrated by domain maps for the three-month averages: January–March (a, e, i, m, q), April-June (b, f, j, n, r), July–September (c, g, k, o, s), and October–November (d, h, l, p, t). The median surface elevation is depicted with black colour.

Figure 4: Geographical zonal distribution of the conditional dust extinction coefficient values (Mm^{-1}) measured by CALIPSO dust product for the regions 10° W to 20° W (a-d), 0° to 10° W (e-h), 0° to 10° E (i-l), 10° E to 20° E (m-p), and 20° E to 30° E (q-t) for the latitudinal regions from 10° N-60° N as illustrated by domain maps for the three-month averages: January–March (a, e, i, m, q), April-June (b, f, j, n, r), July–September (c, g, k, o, s), and October–November (d, h, l, p, t). The median terrain elevation is depicted with black colour.

Figure 5: Geographical zonal distribution of the conditional dust particle depolarization ratio measured by CALIPSO for the regions 10° W to 20° W (a-d), 0° to 10° W (e-h), 0° to 10° E (i-l), 10° E to 20° E (m-p), and 20° E to 30° E (q-t) for the latitudinal regions from 10° N-60° N as illustrated by domain maps for the three-month averages: January–March (a, e, i, m, q), April-June (b, f, j, n, r), July–September (c, g, k, o, s), and October–November (d, h, l, p, t). The median terrain elevation is depicted with black colour.

Figure 6: Geographical distribution of the de-seasonalized trends (yr^{-1}) derived from monthly columnar DOD (a) and for five individual layers (b-f), for the period 2007-2015, aggregated over 10° x 10° grid cells. Hatched filled grid cells depict the statistical significance trends with 99% confidence.

Atmos. Chem. Phys. Discuss., doi:10.5194/acp-2016-902, 2016
Manuscript under review for journal Atmos. Chem. Phys.
Published: 24 November 2016

Atmospheric Chemistry and Physics Discussions

Table 1: Quality control procedures and filtering applied in CALIPSO data.

1.	Screen out all features that are not aerosols
2.	Set all clear air profile measurements to 0.0 km^{-1}
3.	Samples below opaque cloud and aerosol layers are removed
4.	Clear-Sky Mode: Only measurements in which no clouds are in the column are considered
5.	Large negative near-surface extinction filter: all level 2 aerosol extinction samples adjacent to the surface having a value less than -0.2 km^{-1} are ignored
6.	Samples where aerosol extinction uncertainty is less than 99.9 km^{-1} are allowed
7.	CAD score: Only features having cloud-aerosol discrimination (CAD) scores between -100 and -20 are used
8.	Only features having extinction QC flag values of 0, 1, 16, or 18 are allowed
9.	Cirrus Fringes: Misclassified cirrus in the upper troposphere, coming from CAD artifacts, are removed
10.	Remove measurements which are contaminated by surface values: extinction values near the surface less than −0.2 km^{-1} are ignored
11.	Undetected surface attached aerosol low bias filter (Changed between CALIPSO L3 version 1 and version 3): samples classified as “clear air” lying beneath the lowest quality screened aerosol layer whose base is below 250 m from the local surface are ignored
12.	Negative signal anomaly mitigation strategy: all level 2 aerosol extinction coefficients within 60 meters of the planetary surface are excluded from level 3 calculations (new in L3 version 3)
13.	All non-dust aerosol types detected in the cell are assigned with a value of 0.0 km^{-1}
	Extra filters with more strict cloud screening:
14.	All profiles having cloud features anywhere in the column are removed
15.	All profiles which fulfil the L3 CALIPSO “CAD score” or “Cirrus fringes” filters are removed

5

Atmos. Chem. Phys. Discuss., doi:10.5194/acp-2016-902, 2016
Manuscript under review for journal Atmos. Chem. Phys.
Published: 24 November 2016

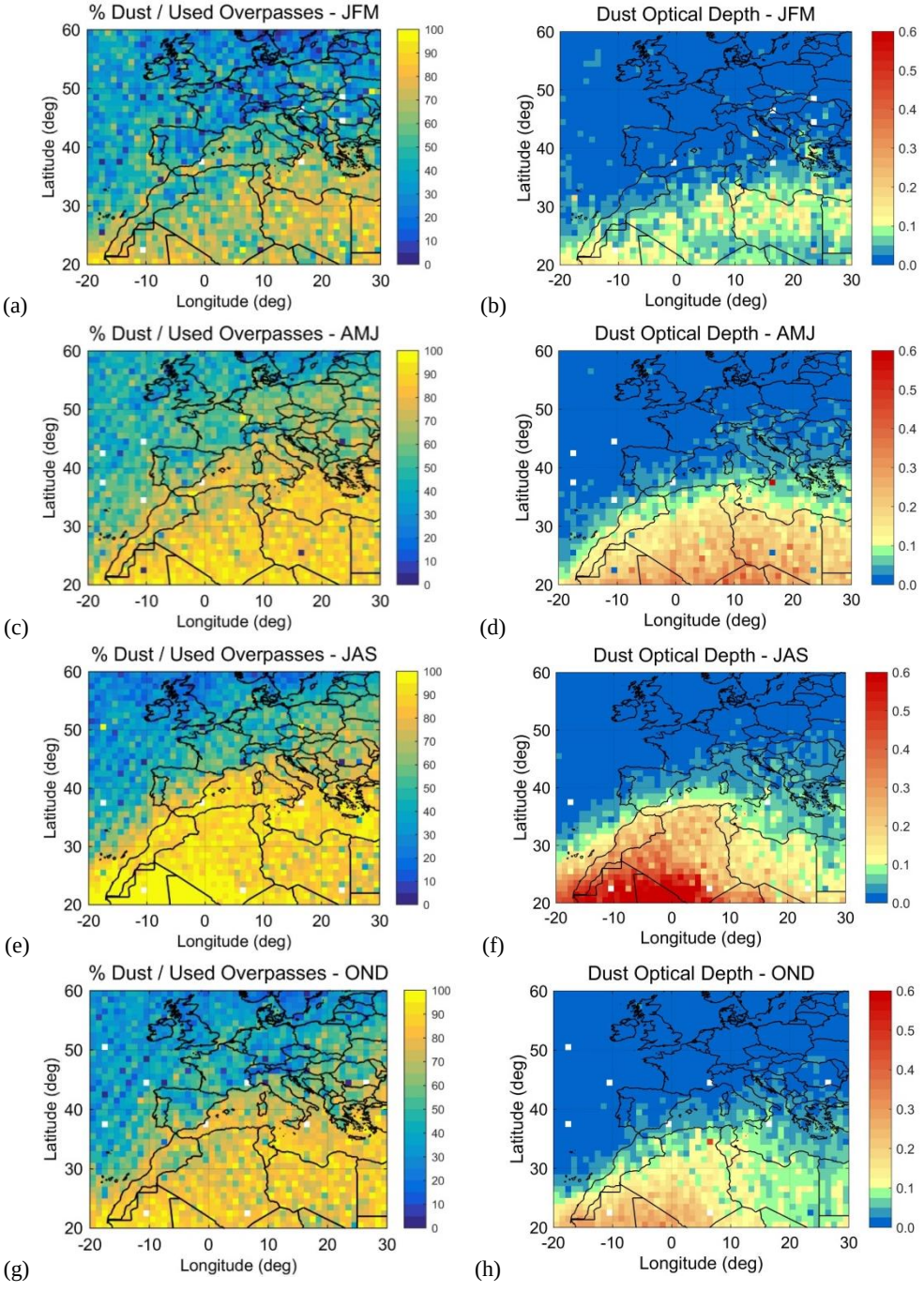

Fig.1

Atmos. Chem. Phys. Discuss., doi:10.5194/acp-2016-902, 2016
Manuscript under review for journal Atmos. Chem. Phys.
Published: 24 November 2016

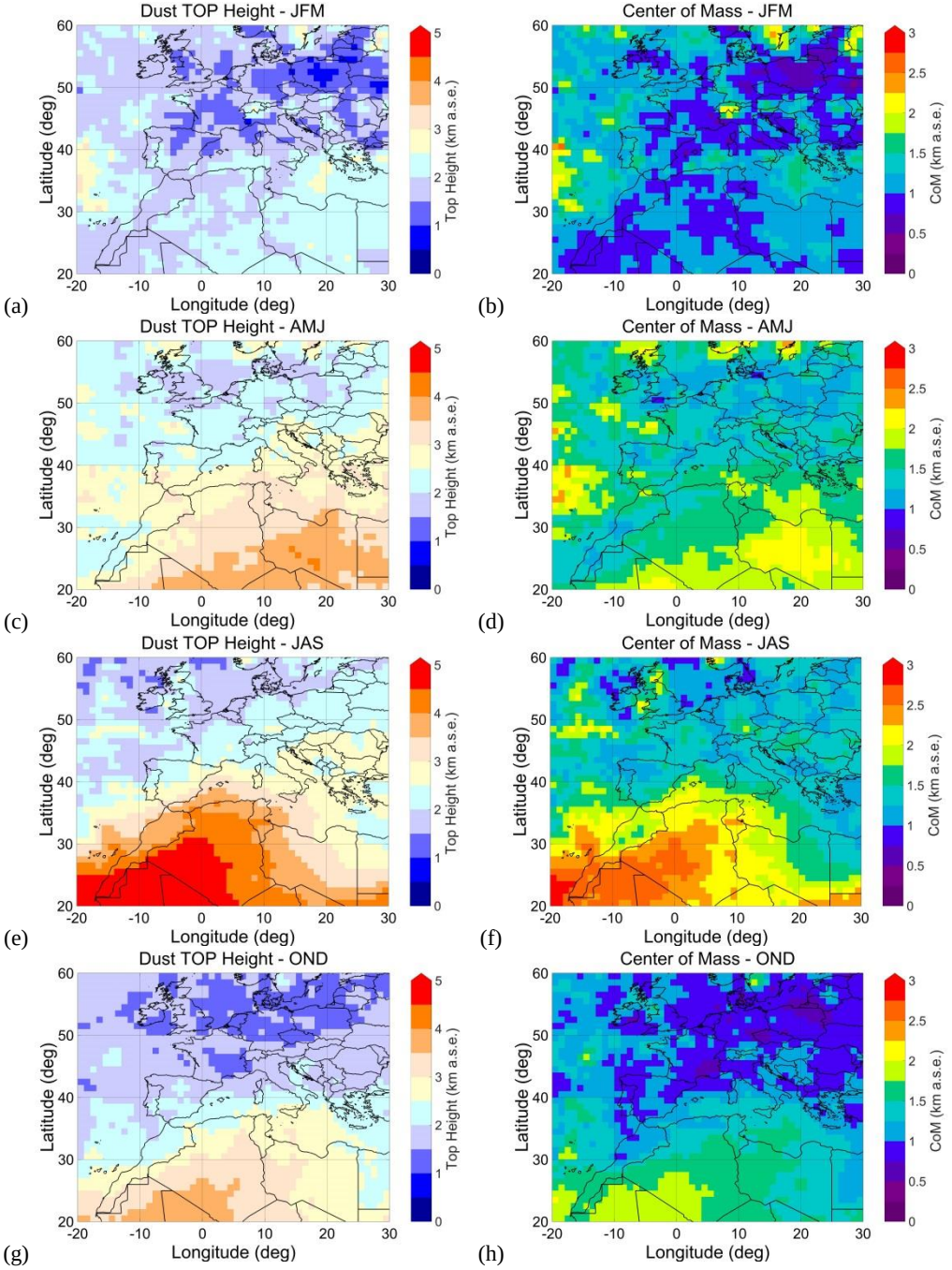

Fig.2

Atmos. Chem. Phys. Discuss., doi:10.5194/acp-2016-902, 2016
Manuscript under review for journal Atmos. Chem. Phys.
Published: 24 November 2016

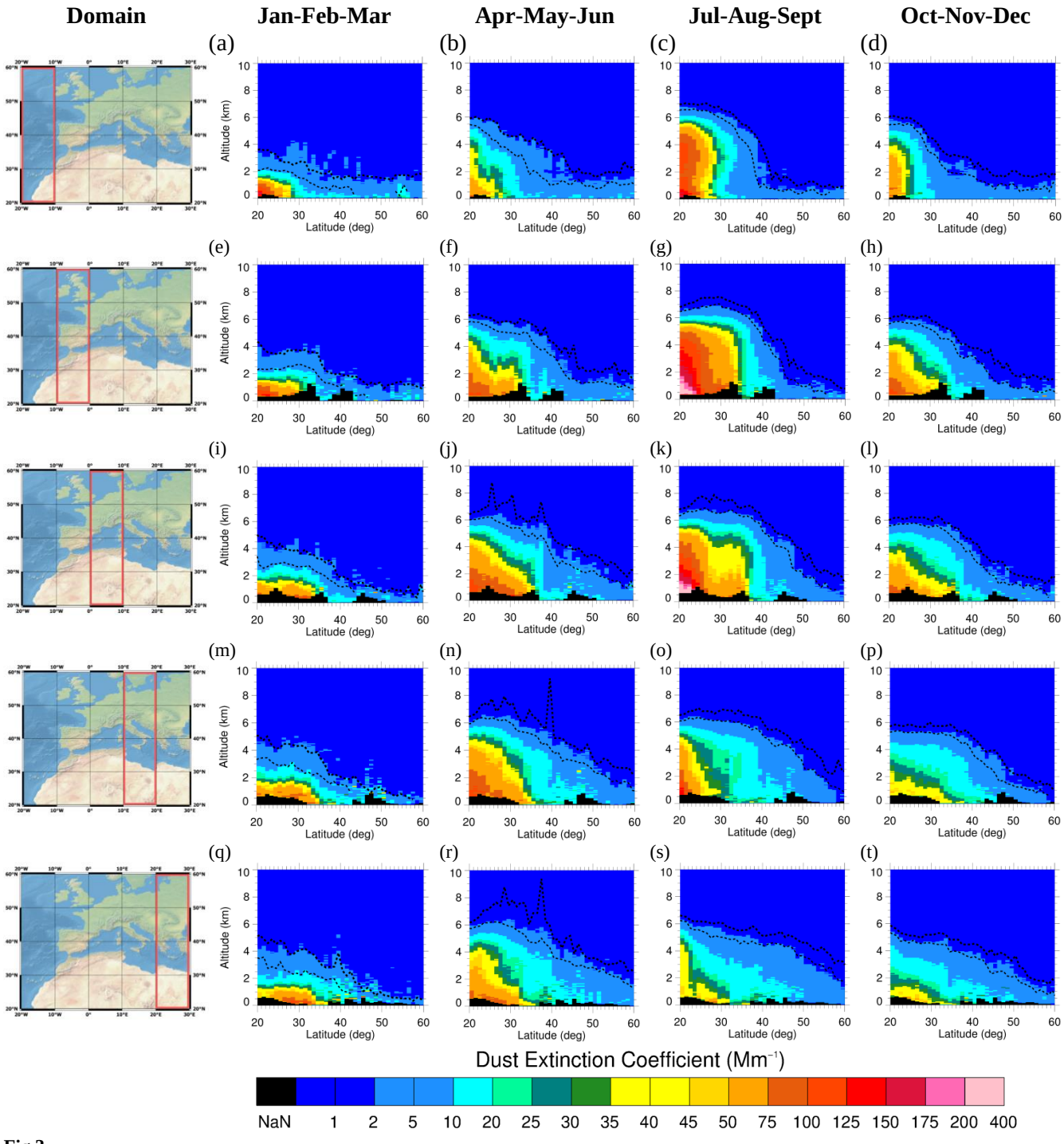

Fig.3

Atmos. Chem. Phys. Discuss., doi:10.5194/acp-2016-902, 2016
Manuscript under review for journal Atmos. Chem. Phys.
Published: 24 November 2016

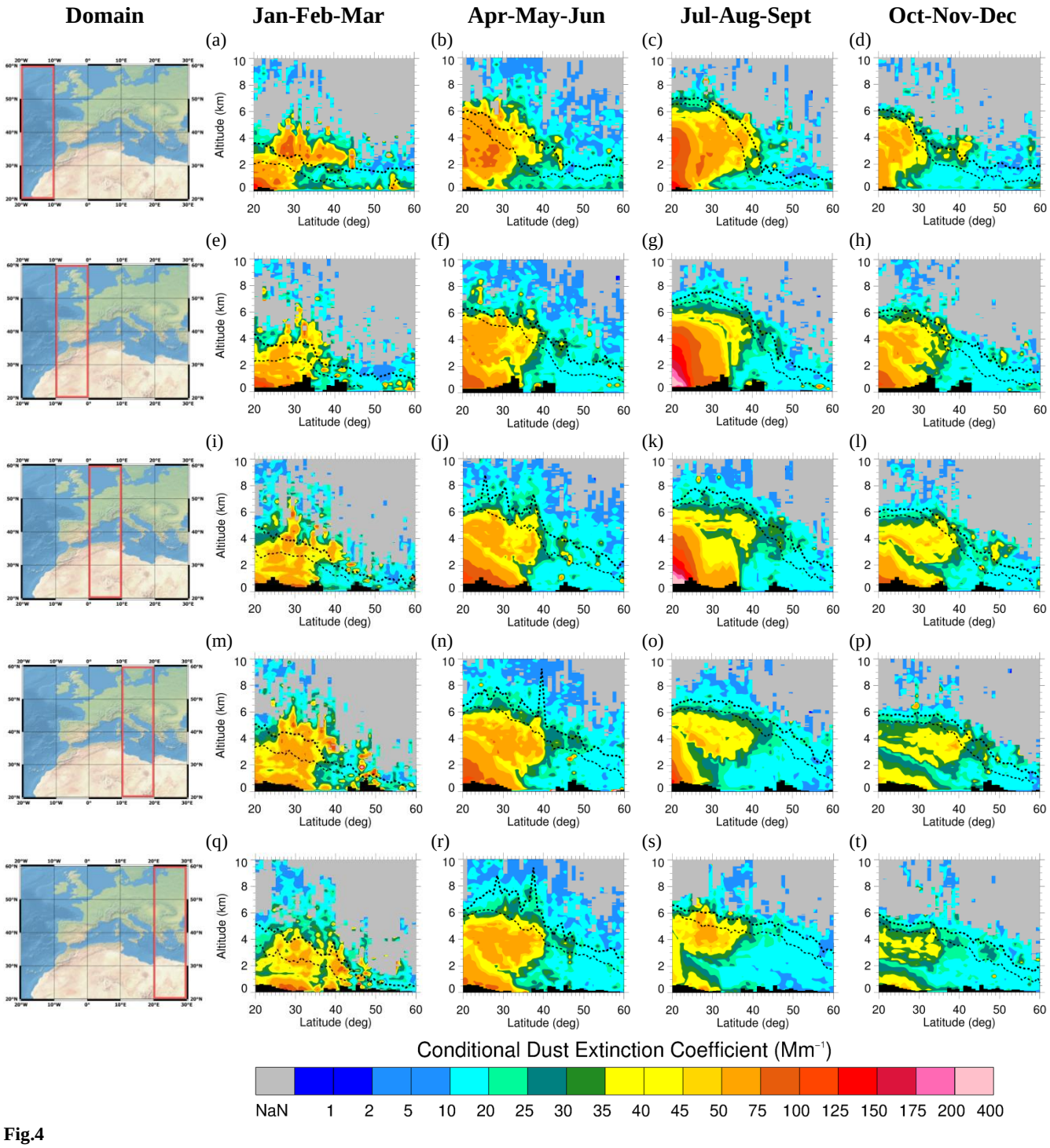

Fig.4

Atmos. Chem. Phys. Discuss., doi:10.5194/acp-2016-902, 2016
Manuscript under review for journal Atmos. Chem. Phys.
Published: 24 November 2016

Atmospheric Chemistry and Physics Discussions

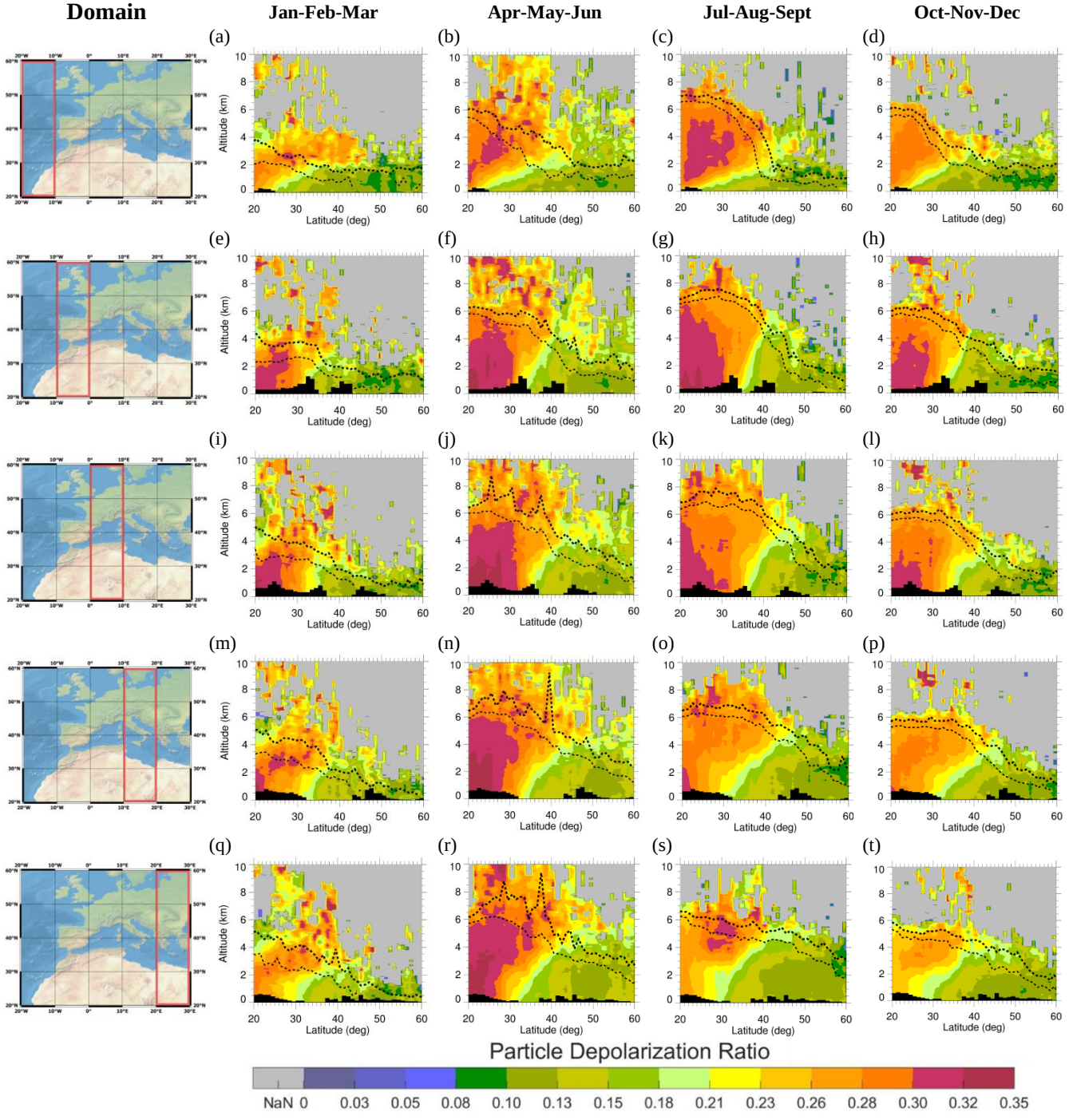

Fig.5

Atmos. Chem. Phys. Discuss., doi:10.5194/acp-2016-902, 2016
Manuscript under review for journal Atmos. Chem. Phys.
Published: 24 November 2016

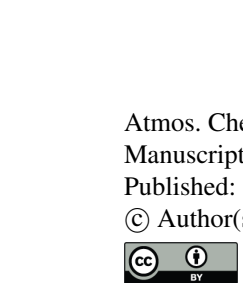

Atmospheric Chemistry and Physics Discussions

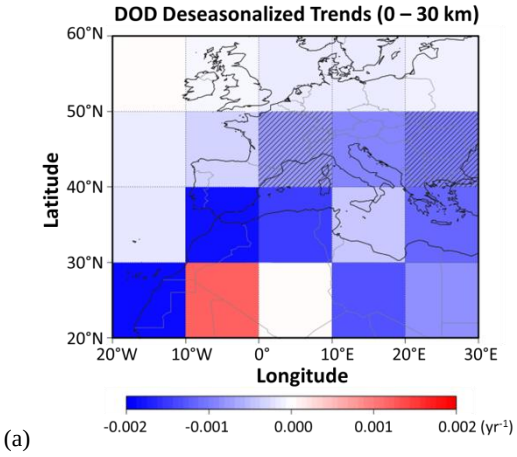

(a)

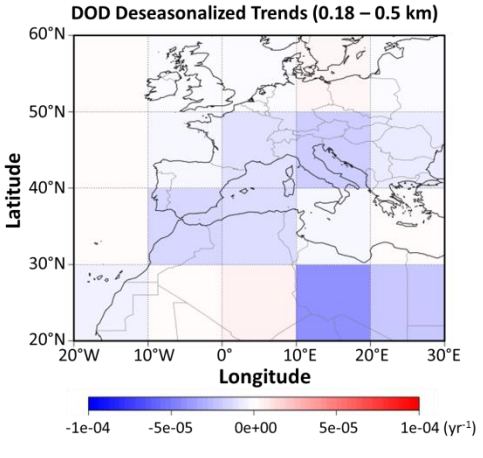

(b)

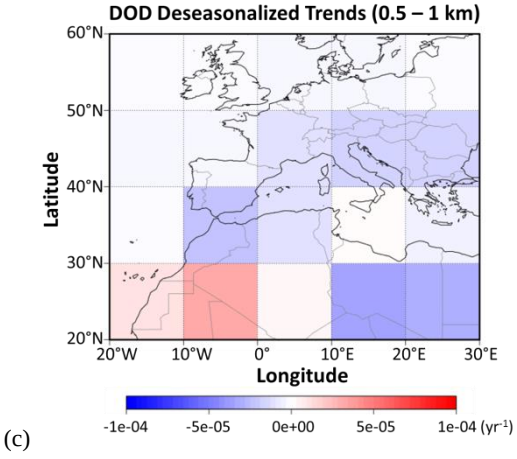

(c)

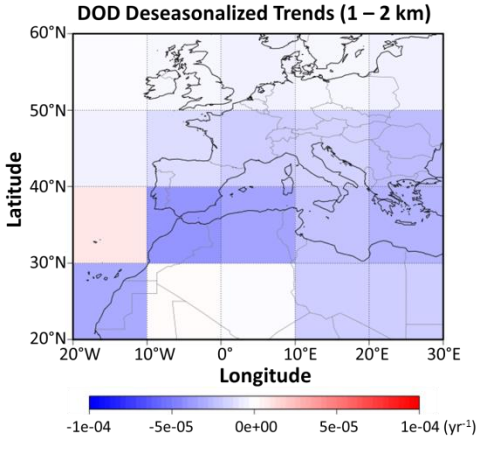

(d)

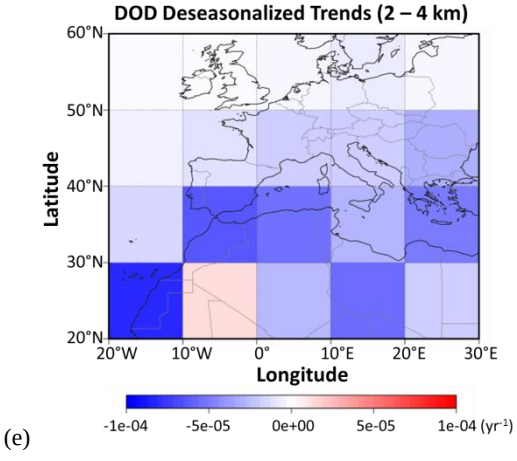

(e)

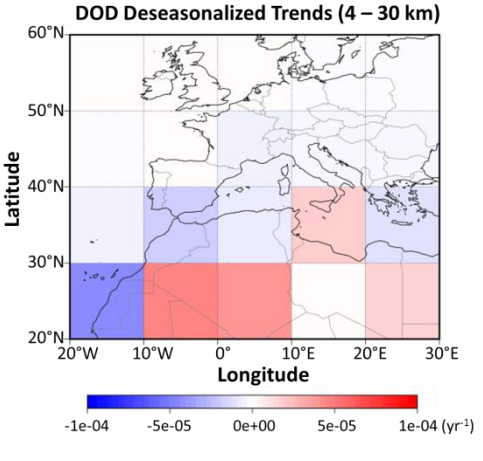

(f)

Fig.6